LLNL-POST-643038

Simulations of Turbulence in Tokamak Edge and Effects of Self-Consistent Zonal Flows *

Bruce I. Cohen and Maxim V. Umansky
Lawrence Livermore National Laboratory
Livermore, CA 94551

With acknowledgments for assistance from

William Nevins, and Mike Makowski
Lawrence Livermore National Laboratory
Livermore, CA 94551

Jose Boedo and Dmitry Rudakov, UC San Diego, San Diego, CA

George McKee and Zheng Yan
University of Wisonsin-Madison, Madison, Wisconsin

Rich Groebner and DIII-D Collaboration, General Atomics
La Jolla, CA

This work was performed under the auspices of the U.S. Department of Energy by Lawrence Livermore National Security, LLC, Lawrence Livermore National Laboratory under Contract DE-AC52-07NA27344

Comparison of BOUT Simulations of Drift Resistive Ballooning Turbulence to Measurements in the Edge of DIII-D L-mode Discharges

1. **Introduction -- Overview, definitions of suite of BOUT simulations and equations used**
2. **BOUT simulations of shot #119919 (with Te & with/without Ti fluctuations)**
3. **Plunging probe data for shot #119919 and comparison to BOUT simulation**
4. **BES data for shot #119919, GKV software synthetic diagnostic adjustment for spatial resolution of BES, and comparison to BOUT simulation**
5. **Inclusion of model $E_{radial}(r)$ fitted to probe and CER data in BOUT simulations of #119919: sheared E_{radial}xB is stabilizing**
6. **Summary of comparisons between BOUT and experimental data from probe and BES for shot #119919**
7. **Simulations of colder, lower density shot #119934, with and without E_{radial}**
8. **New results from LAPD simulation with/without Reynolds stress zonal flow and BOUT simulations of DIII-D with zonal flows (work in progress)**
9. **Conclusions**

BOUT Simulations of Resistive Drift Ballooning Turbulence in Edge Region for DIII-D L-Mode Shots #119919/..21/..30/..34

B.I. Cohen, M.V. Umansky, et al., Phys. Plasmas **20**, 055906 (2013)

- Simulations of electromagnetic resistive drift ballooning in DIII-D L-mode shots #119919, 119921 119930, and 119934, with full geometry and magnetic shear, crossing the separatrix
- Nonlinear BOUT equations for ion density, vorticity, electron and ion velocities, electron and ion temperatures, Ohm's law, and Maxwell's equations.
- In earlier work, we have suppressed a spatial odd-even numerical mode that balloons along field line
- **Simulation results for various physics models and validation against probe and BES data**
- **BOUT obtains steady-state turbulence with fluctuation amplitudes and transport that compare reasonably to DIII-D probe and BES data. Sheared rotation due to $E_{radial}(r)$ is stabilizing, at least linearly.**

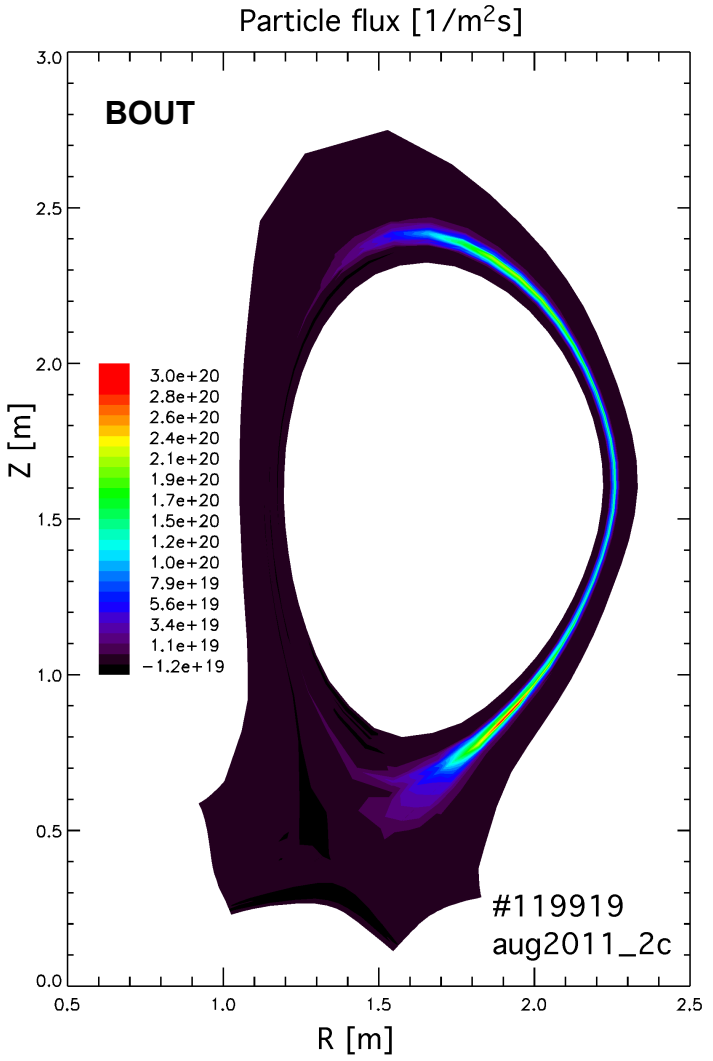

BOUT Simulation of Resistive Drift Ballooning Turbulence for DIII-D L-mode Shots - Outline

- Electromagnetic simulations of resistive ballooning turbulence in single-null DIII-D geometry (Braginskii equations + drift ordering):
  - **Case #1:** No T_e fluctuations, (**a**) with E_r
  - **Case #2:** With T_e fluctuations
  - **Case #3:** With T_e fluctuations and electron parallel thermal conduction
  - **Case #4:** With T_e fluctuations, electron parallel thermal conduction, and $\nabla_{||} = \mathbf{b}_0 \cdot \nabla + \tilde{\mathbf{b}} \cdot \nabla$ in $-\nabla_{||}\phi$ and $\nabla_{||} j_{||}$
  - **Case #5:** With T_e and T_i fluctuations, etc.
  - **Case #6:** With T_e and T_i fluctuations,etc., and imposed (**a**) E_r & (**b**) $5E_r$
- Comparison to probe and BES data for DIII-D shots #119919,21,30,34. These shots are well-characterized L-mode shots exhibiting steady-state turbulence. *B.I. Cohen, M.V. Umansky, et al., Phys. Plasmas **20**, 055906 (2013)*

Case #5: Include Nonlinear Advection of $T_{e,i}$ in BOUT06 Equations for Resistive Drift Ballooning with Magnetic Flutter

- Consider the following simplified Braginskii + reduced Maxwell eqns with drift ordering in the BOUT06 framework:

$$\frac{d\tilde{N}_i}{dt} + \nabla N_i \tilde{V}_{\|} = \left(\frac{2c}{eB}\right) b_0 \times \kappa \bullet (\nabla \tilde{P}_e - N_i e \nabla \varphi) + \nabla_{\|}(\tilde{j}_{\|}/e)$$

$$\frac{d\varpi}{dt} = 2\omega_{ci} b_0 \times \kappa \bullet \nabla \tilde{P} \quad + \quad N_{i0} Z_i e \frac{4\pi V_A^2}{c^2} \nabla_{\|} \tilde{j}_{\|}$$

$$\frac{d\tilde{V}_{\|e}}{\partial t} = -\frac{e}{m_e} E_{\|} - \frac{1}{N_{i0} m_e} (T_{e0} \nabla_{\|} \tilde{N}_i) + 0.51 \nu_{ei} \tilde{j}_{\|}$$

$$\frac{d\tilde{V}_{\|i}}{dt} = -\frac{1}{N_{i0} M_i} \nabla_{\|} \tilde{P},$$

$$\frac{d\tilde{T}_{e,i}}{dt} = \frac{2}{3N_{i0}} \nabla \bullet \left(\kappa_{\|}^{e,i} \nabla_{\|} \tilde{T}_{e,i}\right), \quad \kappa_{\|}^{e} = 3.2 \frac{N_{i0} T_{e0} \tau_{e0}}{m_e}, \; \kappa_{\|}^{i} = \ldots$$

$$\mathbf{E} = -\tfrac{1}{c}\tfrac{\partial}{\partial t}\mathbf{A}_{\|} - \nabla\varphi, \quad -\nabla_{\perp}^2 \mathbf{A}_{\|} = \tfrac{4\pi}{c}\mathbf{j}_{\|}, \quad \mathbf{B} = \nabla \times \mathbf{A}_{\|} + \mathbf{B}_0$$

$$\varpi = \nabla \cdot \left[eZ_i N_i \nabla\varphi\right] + \nabla_{\perp}^2 P_i \approx eZ_i N_{i0} \nabla^2 \varphi \qquad \nabla_{\|} = \mathbf{b}_0 \cdot \nabla + \tilde{\mathbf{b}} \cdot \nabla \qquad Z_i = 1$$

$$\frac{d}{dt} = \frac{\partial}{\partial t} + (\mathbf{V}_{E0} + \tilde{\mathbf{V}}_E) \bullet \nabla \quad N_i = N_{i0} + \tilde{N}_i, \quad T_s = T_{s0} + \tilde{T}_s, \ldots$$

$$\tilde{P} = N_{i0}(\tilde{T}_e + \tilde{T}_i) + \tilde{N}_i (T_{e0} + T_{i0}), \quad T_{i0} = T_{e0}, \quad V_{\|s0} = 0$$

- Electromagnetic with $\nabla_{\|} = \mathbf{b}_0 \cdot \nabla + \tilde{\mathbf{b}} \cdot \nabla$ in $-\nabla_{\|}\phi$ and $\nabla_{\|}\tilde{j}_{\|}$
- Actual DIII-D geometry
- Radial bdry conditions: Von Neumann on fluid fluctuations, Dirichlet on $A_{\|}$ & ϕ

  Fluctuations decay to 0 at outer bdry & not necessarily at inner bdry
- DIII-D - like fixed background profiles for shots #119919 and 119934
- Case #4 includes T_e fluctuations (not T_i fluctuations) and parallel heat conduction
- Case #5 includes all of the above

History of rms fluctuation amplitudes in midplane at separatrix with electron parallel thermal conduction and magnetic flutter, showing saturated turbulence in BOUT for shot #119919

BOUT Cases 4 and 5

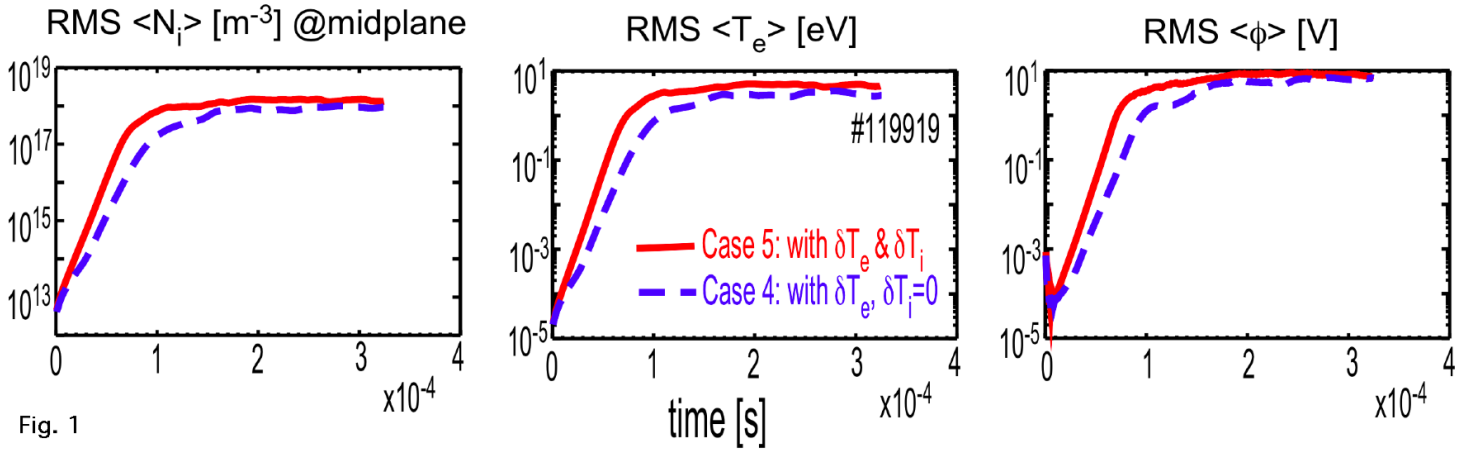

Fig. 1

- With T_e (& T_i) fluctuations, electron parallel thermal conduction, convective nonlinearities, and

$$\nabla_{||} = \mathbf{b}_0 \cdot \nabla + \tilde{\mathbf{b}} \cdot \nabla \text{ in } -\nabla_{||}\phi \text{ and } \nabla_{||} j_{||}$$

- Temperature and density fluctuations saturate

- Including T_i fluctuations increases fluctuation amplitudes modestly

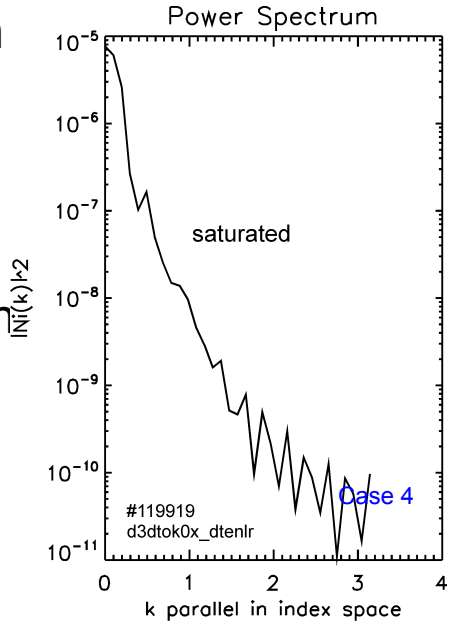

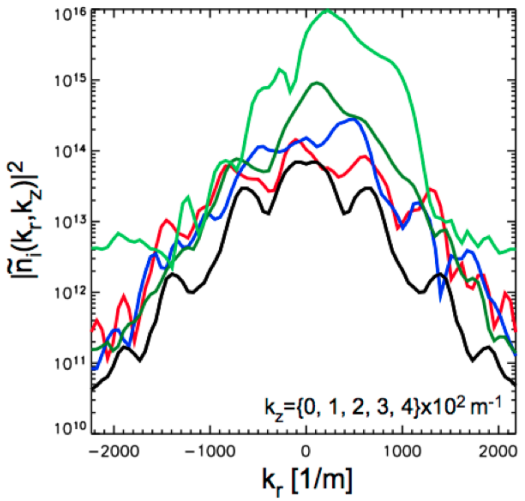

Fig. 9

Time-averaged ion density fluctuations in the midplane saturate at ~10-30% and peak near R_{sep}

BOUT Cases 4 and 5

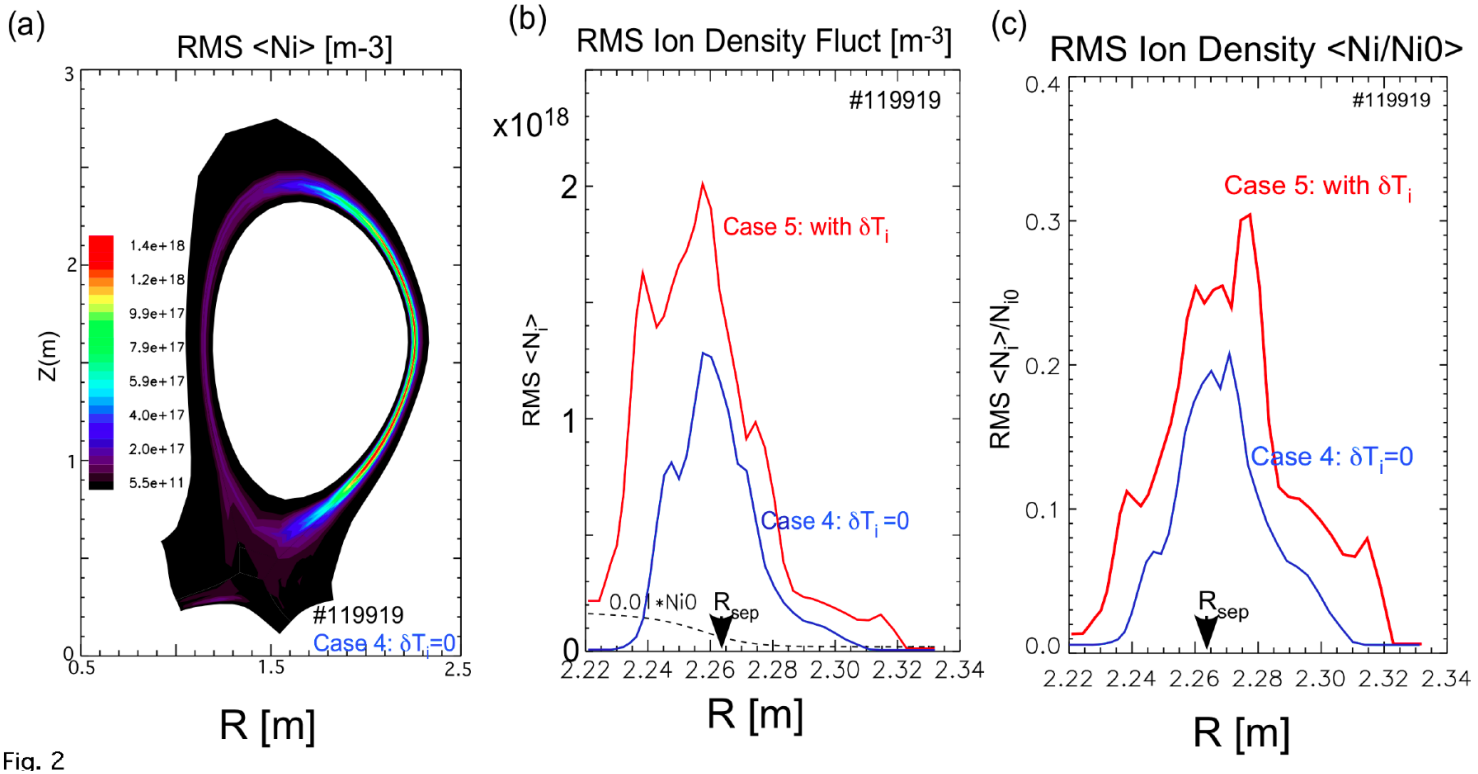

Fig. 2

- With T_e fluctuations, electron parallel thermal conduction, and $\nabla_{\parallel} = \mathbf{b}_0 \cdot \nabla + \tilde{\mathbf{b}} \cdot \nabla$
- Including T_i fluctuations leads to higher fluctuation amplitudes
- There is a poloidal asymmetry wrt midplane in the fluctuations

Ballooning Nature of Turbulence, Case 1 #119919

BOUT Case 1

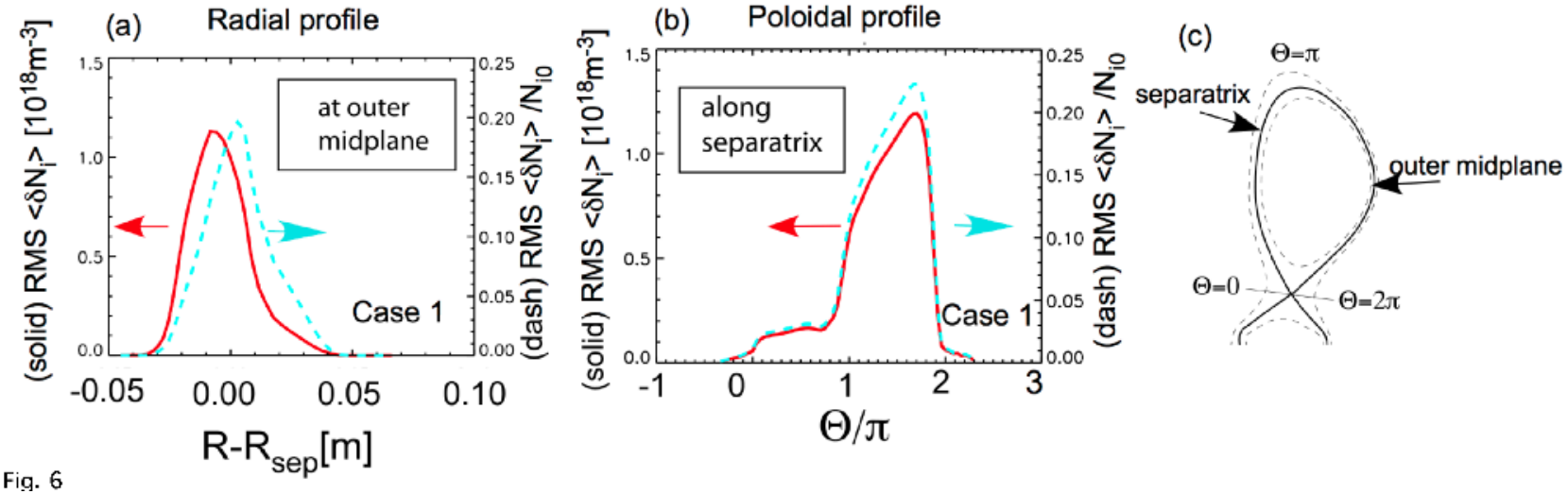

Fig. 6

- The fluctuations are radially localized near the separatrix
- The fluctuations balloon to the outer side of torus where the pressure-weighted curvature drive is strongest

Time-averaged T_e fluctuations in the midplane peak near the R_{sep} and saturate at ~50-150% relative amplitude at $R>R_{sep}$

BOUT Cases 4 and 5

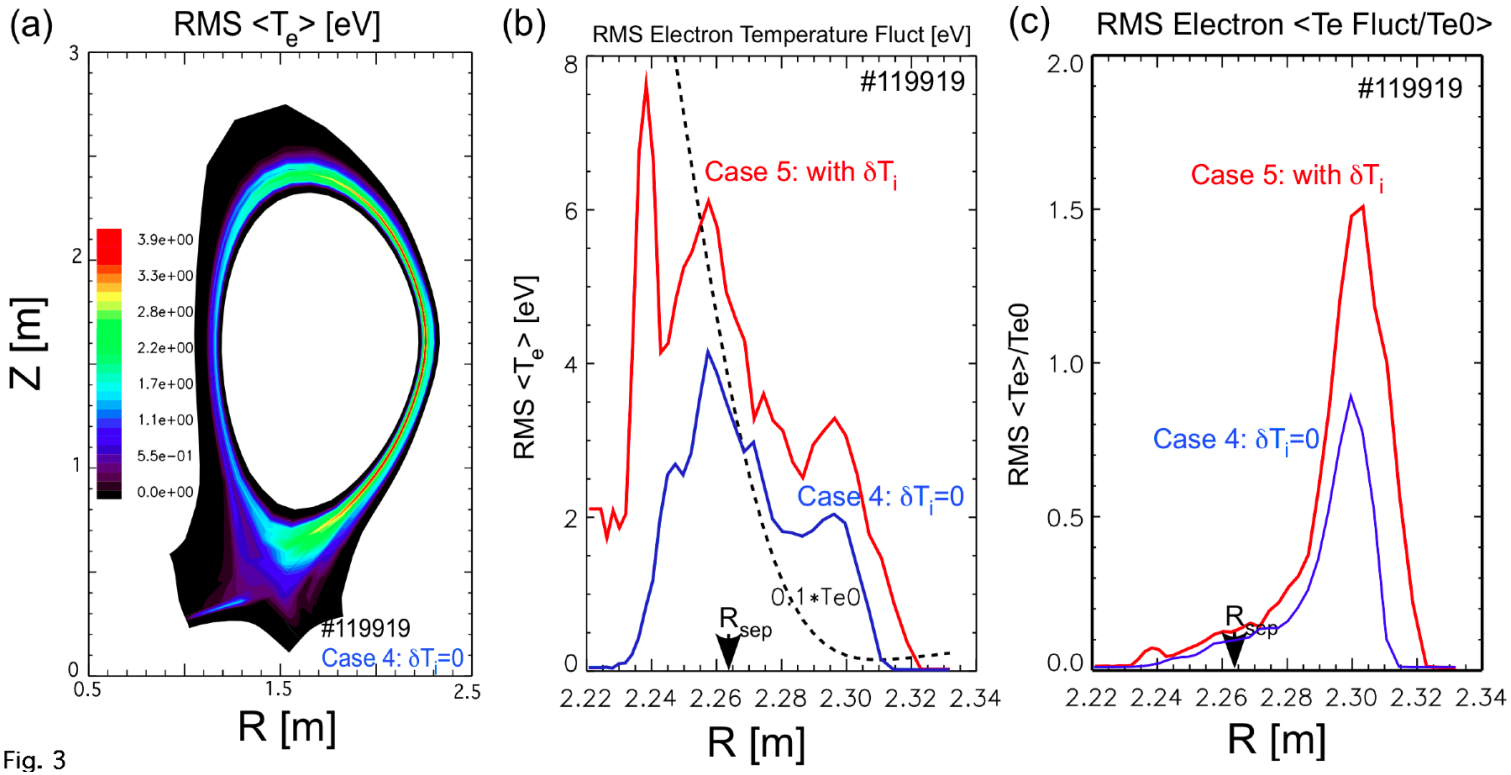

Fig. 3

- With T_e fluctuations, electron parallel thermal conduction, nonlinear convection, and $\nabla_{\parallel} = \mathbf{b}_0 \cdot \nabla + \tilde{\mathbf{b}} \cdot \nabla$
- T_e fluctuations are ~10% near R_{sep} and are higher with finite T_i fluctuations

B. Cohen & Umansky, BOUT++2013 Workshop

Time-averaged ion particle diffusion coefficient in the midplane saturates at ~1.5-2 m^2/s

BOUT Cases 4 and 5

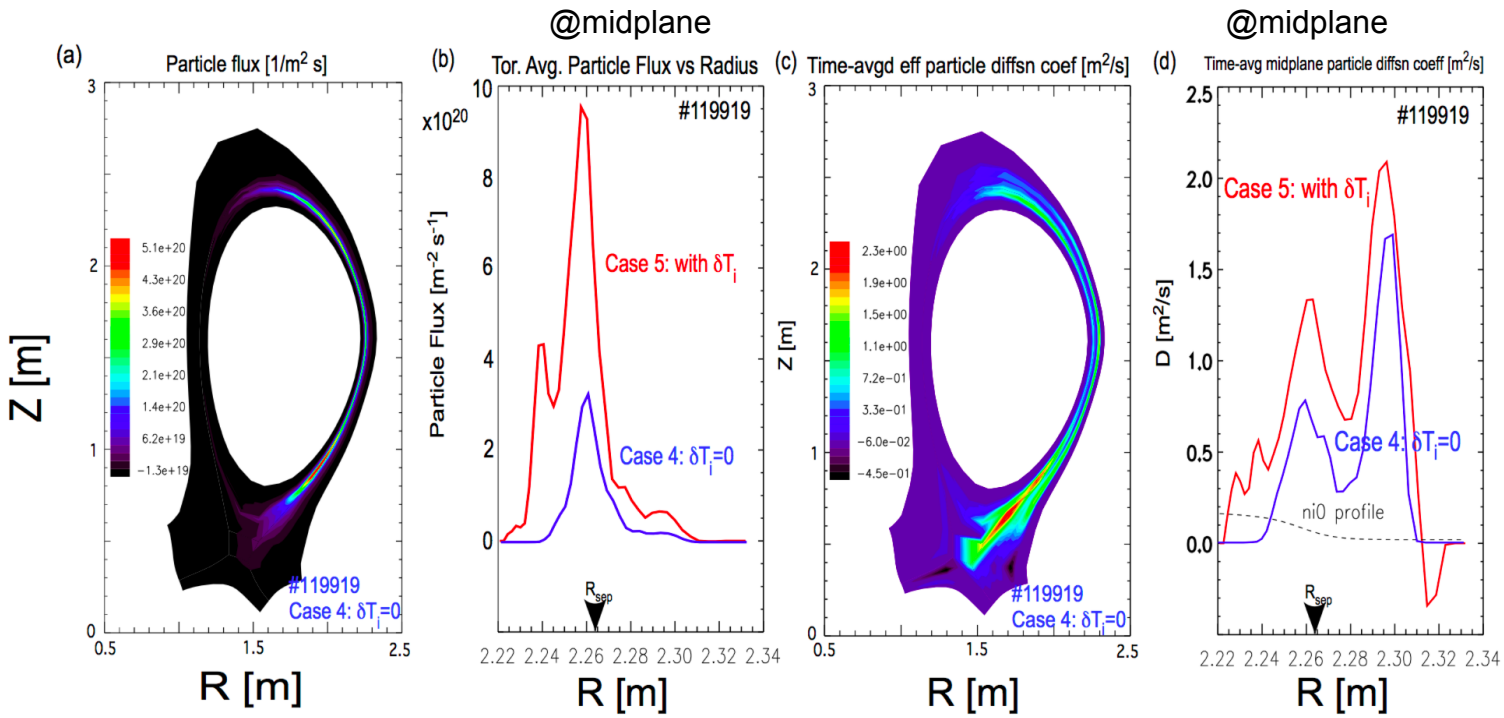

- With T_e fluctuations, electron parallel thermal conduction, nonlinear convection, and $\nabla_{\parallel} = \mathbf{b}_0 \cdot \nabla + \tilde{\mathbf{b}} \cdot \nabla$
- Including T_i fluctuations leads to higher particle fluxes and diffusion coefficient

Time-averaged electron conductive thermal diffusion coefficient in the midplane saturates at ~2-6 m^2/s

BOUT Cases 4 and 5

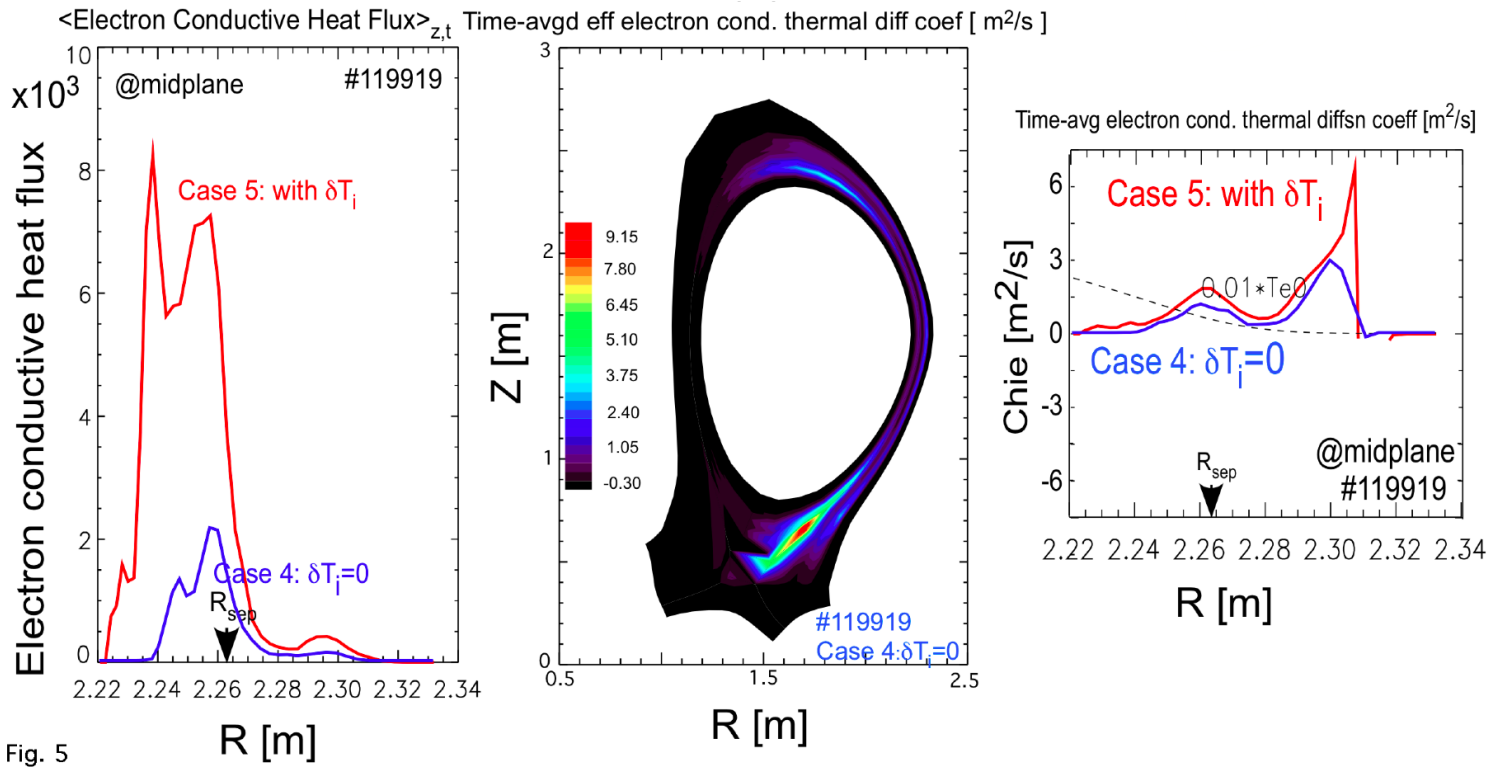

Fig. 5

Note: Here heat flux (conductive) = $\frac{3}{2} N_0 < \delta v_r \delta T_e >_{tor,t}$, and $\chi_e = -\frac{3}{2} N_0 < \delta v_r \delta T_e >_{tor,t} / N_0 \nabla T_{e0}$

- With T_e fluctuations, electron parallel thermal conduction, nonlinear convection, and $\nabla_{\|} = \mathbf{b}_0 \cdot \nabla + \tilde{\mathbf{b}} \cdot \nabla$
- Including T_i fluctuations leads to higher heat fluxes and diffusion coefficient

There is reasonable agreement between BOUT simulation and Langmuir probe data for DIII-D #119919 with respect to peak fluctuation amplitudes, particle and thermal flux, and localization

- BOUT with T_e & T_i fluct' ns, electron parallel thermal conduction, convective nlrity, $\nabla_{\parallel} = \mathbf{b}_0 \cdot \nabla + \tilde{\mathbf{b}} \cdot \nabla$

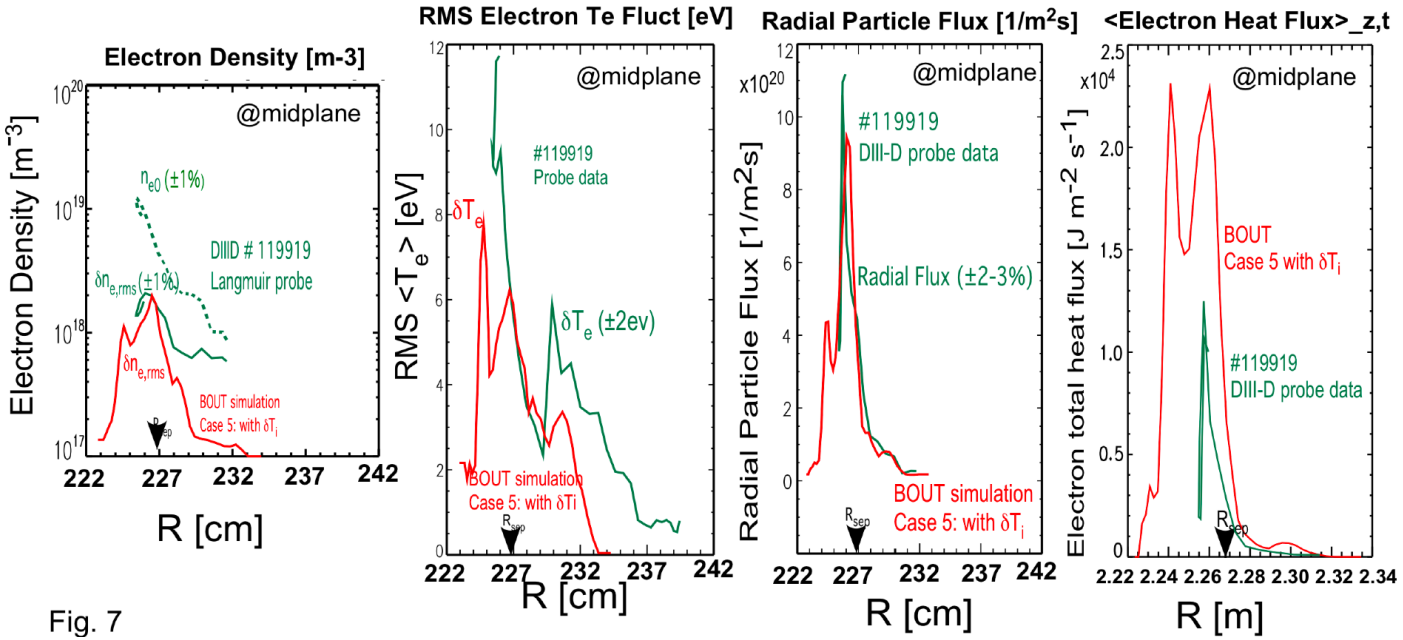

Fig. 7

- Probe signals decrease below noise levels for R > 231 cm, and stop for R < 225 cm
- Typical experimental rms δn_e and δT_e fluctuations at the separatrix exceed ~20% & ~50%
- δn_e, δT_e and the probe fluxes in the midplane usually peak near the separatrix
- BOUT simulations and Langmuir probe data agree within factors of 2 in peak amplitudes and localization for 2.25m ≤ R ≤ 2.31m

Reasonable Agreement between BOUT Simulation and Beam Emission Spectroscopy Data for DIII-D #119921 with respect to Peak Fluctuation Amplitude, Localization, Spatial Correlation Width, and Spectral Width

ñ/n Amplitude Profile | **Spatial Correlation** | **Density Fluctuation Spectrum**

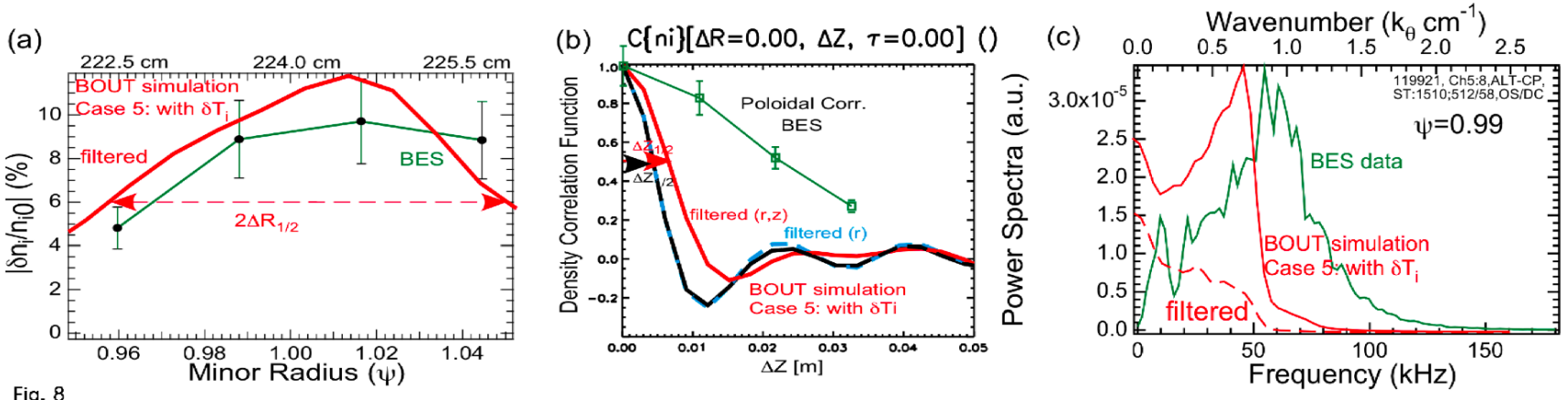

Fig. 8

@outer midplane

- Spatial filtering (1D or 2D) is required in simulation diagnostics to model the 1 cm limit on spatial resolution in the BES grid in R and Z.
- Spatial filtering of the BOUT diagnostics reduces and spatially spreads peaks
- There is agreement between BOUT and BES to within factors of two or three, or better

Philosophy on the Modeling of Sheared Radial Electric Field and Zonal Flow Effects

- Sheared ExB flows can reduce linear growth rates and saturated turbulence levels for drift-type instabilities, e.g., core ITG, L-H transition phenomenology,…
- But zonal flows are not always important, e.g. in the ETG study of Holland et al., Nuc. Fusion **43**, 761 (2003), zonal flows are not an important feature.
- In the edge, $E_r(r)$ is influenced by sheaths at the divertor plates and limiters, by interactions with neutral gas, sources/sinks, other non-ambipolar processes, and the turbulence-generated zonal flows via the Reynolds stress.
- If there is good experimental data for $E_r(r)$ that is sufficiently resolved spatially and temporally, and extends over the whole spatial domain, this data would incorporate all the physics to determine the zonal flows completely.
- We first study the effects of (1) an imposed steady $E_r(r)$ based on fitting to experimental data, (2) $E_r(r,t)$ including the Reynolds stress for all modes except for the longest radial wavelengths of the axisymmetric modes which are held constant at their initial defined values to maintain "equilibrium" profiles (ref. Waltz & Candy), and (3) including evolution of n=0 modes only in the vorticity eqn

Model the Experimental Radial Electric Field to Study the Effects of Imposed E_0xB Shearing on Simulated Turbulence

- An equilibrium radial electric field E_0 is included in BOUT simulations for Cases 1, 4, & 5, using fits to the experimental probe and CER data near the midplane
- L-mode plasmas typically have weakly sheared ExB flows. In our fit to probe and CER data the ExB shearing rate is < 2.4 x 10^4 (1/s) < BOUT growth rates~O(1)x10^5(1/s)
- We expect that with imposed sheared ExB flow there will be weaker linear instability and some reduction of the saturated turbulence

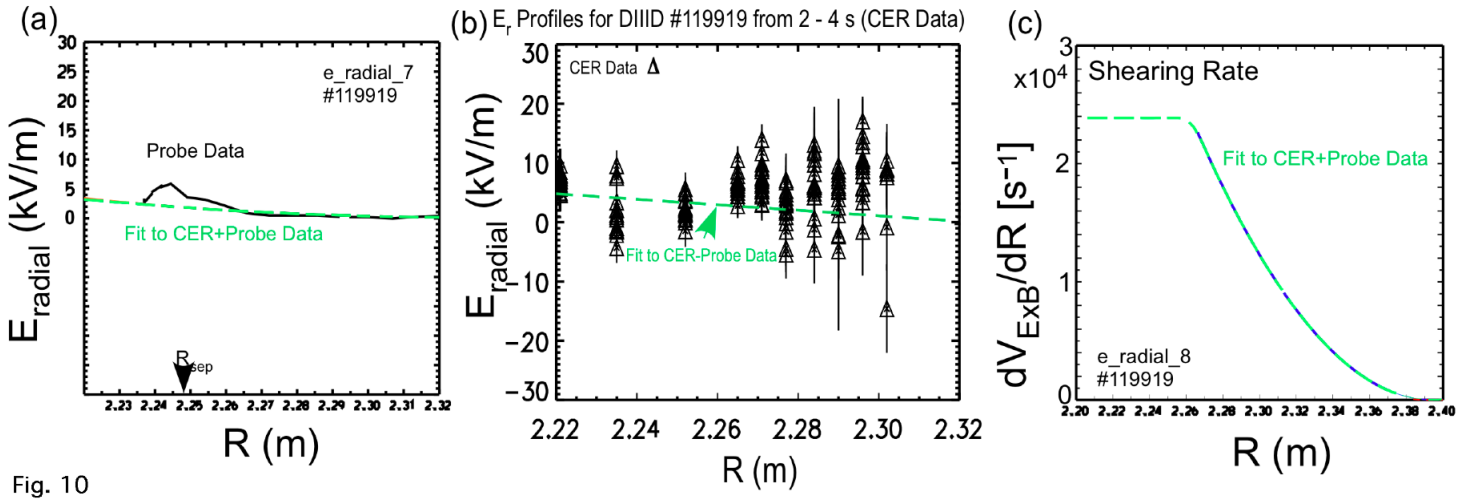

Fig. 10

Fusion Energy Sciences

Imposed E_0xB Shearing Reduces Both Linear Growth Rates and Saturated Turbulent Amplitudes

- An equilibrium radial electric field E_0 is included in BOUT simulations for #119919 **Cases 1, 4, 5, & 6**, using fits to the experimental probe and CER data near midplane
- In our fit to probe and CER data the ExB shearing rate is < 2.4 x 10^4 (1/s) < BOUT growth rates~O(1)x10^5(1/s)
- Imposed sheared ExB flow weakens linear growth rates, and saturation is much delayed (>2ms) and at lower amplitudes, while 5xE_r is much more stabilized.

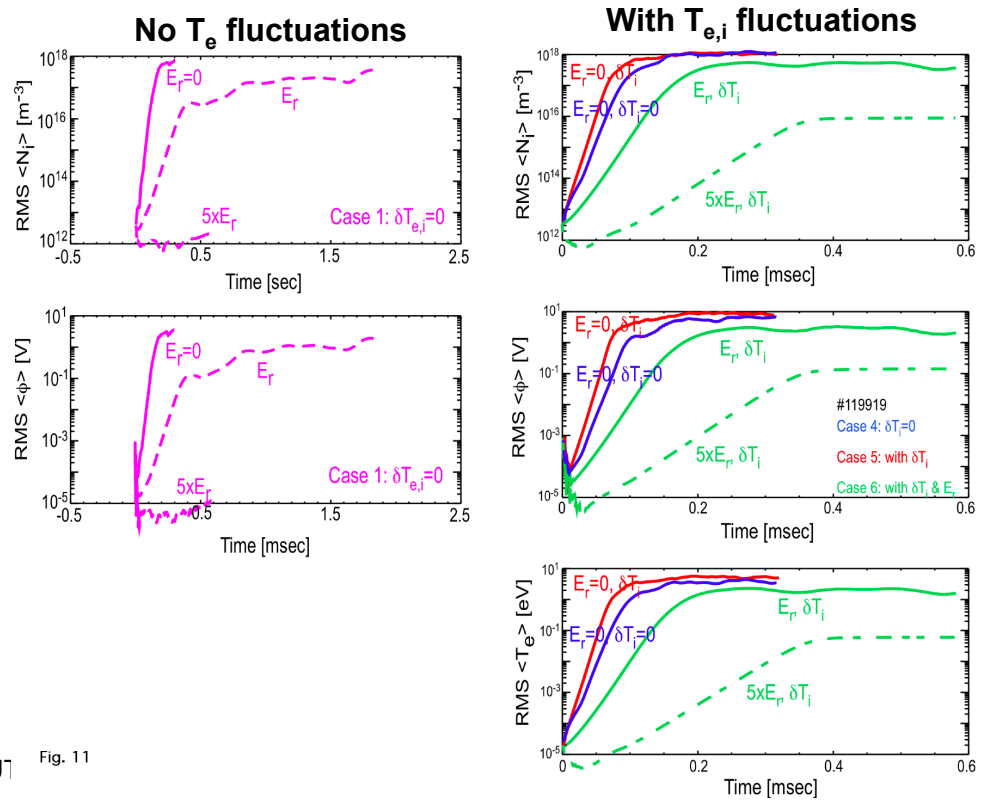

B. Cohen & Umansky, BOUT Fig. 11

Imposed E_0xB Shearing Reduces Both Linear Growth Rates and Saturated Turbulent Amplitudes in Simulations

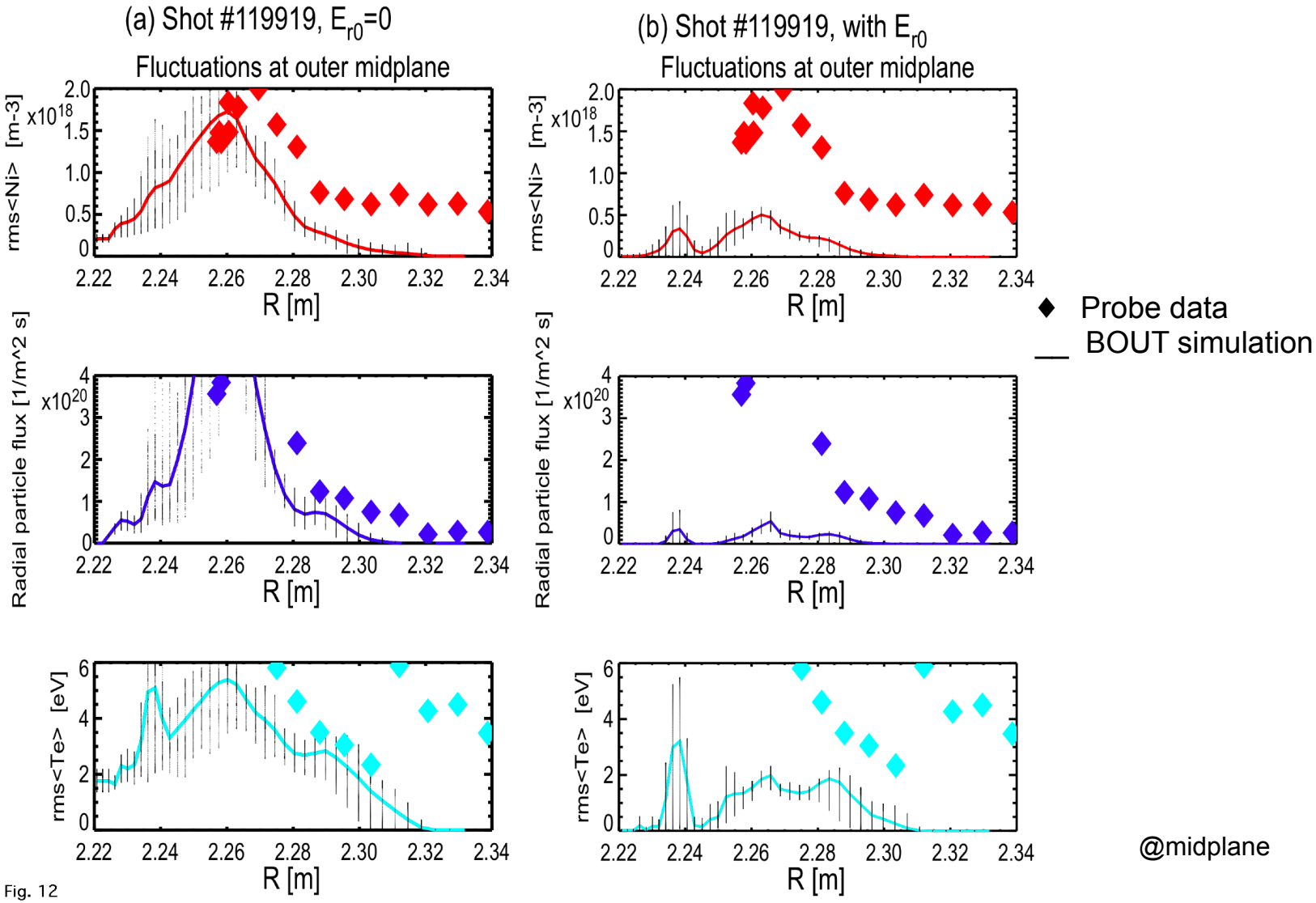

Fig. 12

As the Physics Model Becomes More Complete, the Agreement of BOUT Results with DIII-D Probe Data Improves - Summary

- Comparison of suite of BOUT simulations to shot #119919: peak values in midplane at saturation near R_{sep} (E_{rad}=0, $E_{rad}\neq 0$, $E_{rad}=5E_{rad}$ with δT_e convective nonlinearity)

Bout simulation	$<\delta N_i>_{rms}$ (10^{18} m^{-3})	$<\delta T_e>_{rms}$ (eV)	Radial Particle Flux (10^{20} /m^2 s)	D_r (m^2/s) local	Conductive Radial Heat Flux $=\frac{3}{2}N_0<\delta\tilde{v}_r\delta\tilde{T}_e>$ (10^3 J/m^2 s)	χ_e(m^2/s), local (conductive)
#1: δT_e=0	0.95	N/A	1.8	0.4	N/A	N/A
#1a: w/E_r**	0.37	N/A	0.07	0.02	N/A	N/A
#4: $\delta T_e\neq 0$ $\kappa_{\|e}\neq 0$ & $\tilde{\mathbf{b}}\cdot\nabla$	1.3	4.0	3.3	1.7	3.3	2.7
#5 & w/δT_i	2.0	7.5	9.5	2	10	2.2
#6a w/E_r	0.7	5.5	0.8	0.27	2.5	0.32
#6a w/5E_r	0.3	3.5	0.18	0.035	0.75	0.036
DIII-D #119919 probe data	2.0	10	11.0	~0.2-1 ‡	1.2	~1-2 ‡

**Cases #1 w/E_r has not saturated at end of simulation (1.8 ms)

‡Typical, flux-surface-averaged values for shot #119919 inferred from UEDGE reconstruction

Comparison of BOUT Results with BES Data for Suite of Physics Models - Summary

- Comparison of suite of BOUT simulations to shot #119921 BES data: fluctuation frequency spectra, peak density amplitude radial half-width, correlation lengths
- Factor of 2 or better agreement seen between simulation synthetic diagnostics with filtering and the DIII-D #119921 BES data (with or without sheared E_0xB velocity included in BOUT)

Bout simulation	$\langle \delta N_i/N_i \rangle_{rms}$ peak vs. R raw/filtered	$\Delta R_{half\text{-}max}$ of $\langle \delta N_i/N_i \rangle_{rms}$ (cm) raw/filtered	$\Delta Z_{corr,half\text{-}max}$ of density (cm) raw/filtered	Peak freq in density fluct' t' n spect, raw/filtered (10^5 rad/s)	Freq half-max in density fluct' t' n spect, raw/filtered (10^5 rad/s)
#1: $\delta T_e=0$ **#1a:** w/E_r**	0.13 / 0.07 0.065/0.045	1.2 / 1.5 0.7/0.8	0.6 / 0.9 2.0 / 2.3	3 / 0.5 0 / 0	4 / 2 1/ 0.7
#4: $\delta T_e \neq 0$ $\kappa_{\|e} \neq 0$ & $\tilde{\mathbf{b}} \cdot \nabla$	0.20 / 0.12	1.4 / 1.2	0.4 / 0.7	3.0 / 1.5	2 / 1.2
#5: w/δT_i	0.21 / 0.12	1.7 / 2	0.4 / 0.7	3.0 / 0&1.5	1 / 1.5
#6a: w/E_r **#6b:** E_r=5E_r	0.07 / 0.05 0.011/0.006	1.5 / 1.7 0.5 / 0.6	0.8/ 0.9 3/3	0.5 / 0.5 3.8 / 3.8	0.5 / 0.5 0.25 / 0.25
DIII-D #119921 BES data	0.09 ±0.2	2 ±0.2	2 ±0.2	3.8	1.3 ±0.2

**Cases #1 w/E_r has not saturated at end of simulation (1.8 ms)

Comparison of Probe Data from Shots #119930 and 119934 vs. 119919 -- Edge Plasmas with Lower Density and Temperature

- L-mode shots #119930 and 119934 edge plasmas are colder and have lower densities than in shot #119919
- The growth rate for resistive ballooning is proportional to $\eta^{1/3}\beta^{2/3}/n^{1/3} \propto T^{1/6}n^{1/3}$
- A factor of two lower temperature and density decreases the drive for resistive ballooning by O (1/√2) if all else is fixed in shots #119930/119934 vs. #119919

N_{i0} & T_{e0} profiles

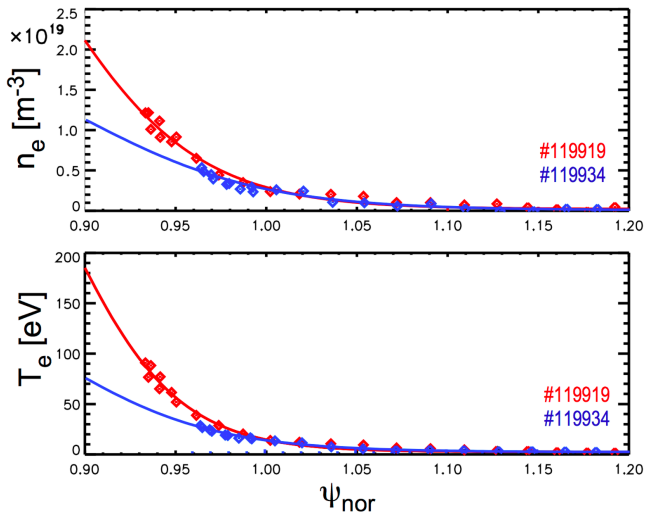

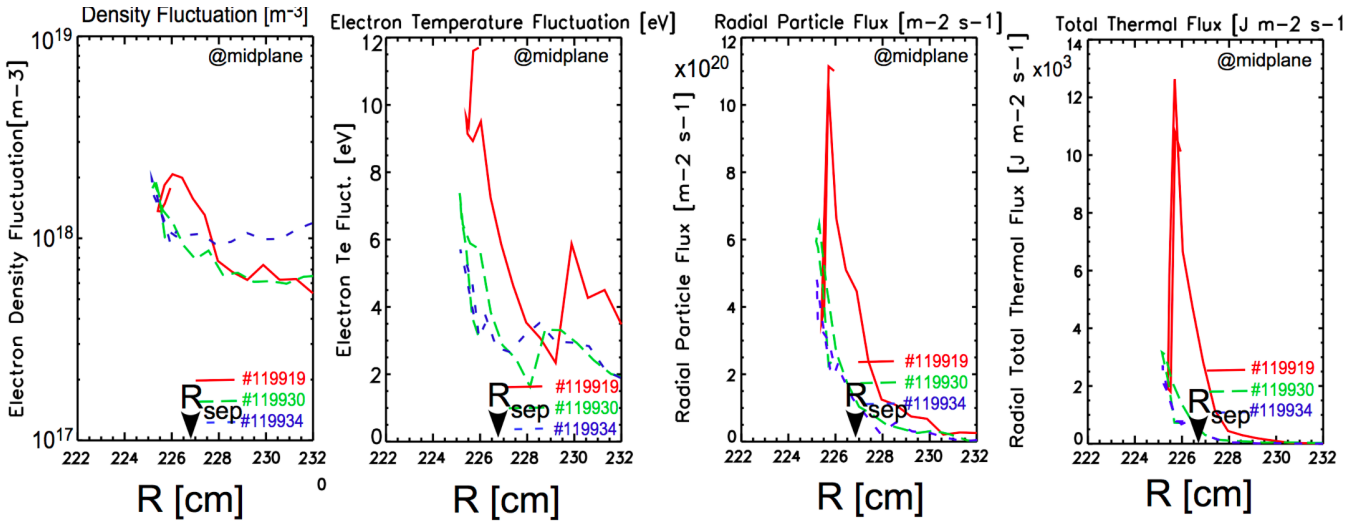

Reduced N_{i0} & T_{e0} lead to **reduced fluctuation amplitudes and radial fluxes** in #119930 & 119934

@midplane

B. Cohen & Umansky, BOUT++2013 Workshop

BOUT Simulations of Shots #119919 and 119934 Show Turbulence Is Reduced at Lower Equilibrium Temperature and Density

@midplane

- BOUT simulations of **Case 5** with no E_{radial} for shots # 119919 and 119934 show that the linear growth rate for the resistive-drift ballooning instability is reduced in 119934, in qualitative agreement with theoretical expectation with its lower equilibrium electron temperature and density in the edge
- The absolute values of the fluctuation amplitudes are reduced in 119934 accompanying the reduction in growth rate of the instability
- Note that cases with temperature fluctuations have increased interchange drive in general and with T_i fluctuations are more unstable than without.

Case 5 #119919,34

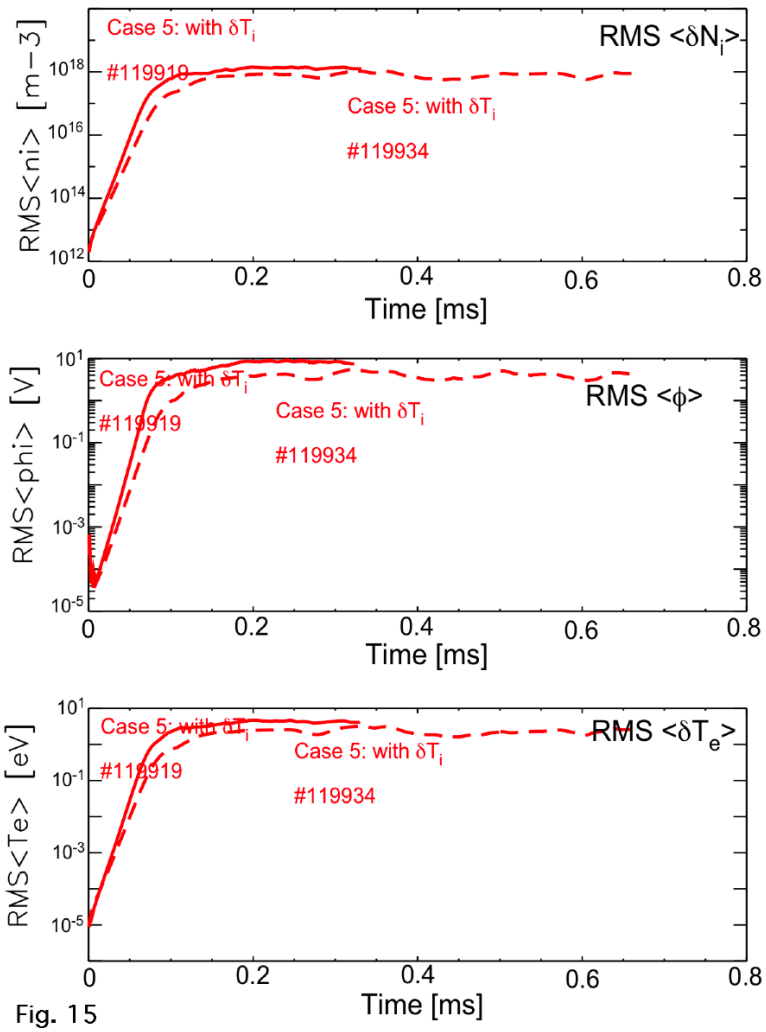

Fig. 15

BOUT Simulation and Probe Data Show that #119934 Is Slightly Less Turbulent Than #119919

- Probe data from L-mode shots #119919 & 34 are compared with BOUT simulations including T_e & T_i fluctuations (**Case 5**). Turbulence in #119934 is slightly reduced from that in #119919
- Density and temperature fluctuations, and radial fluxes tend to peak near the separatrix

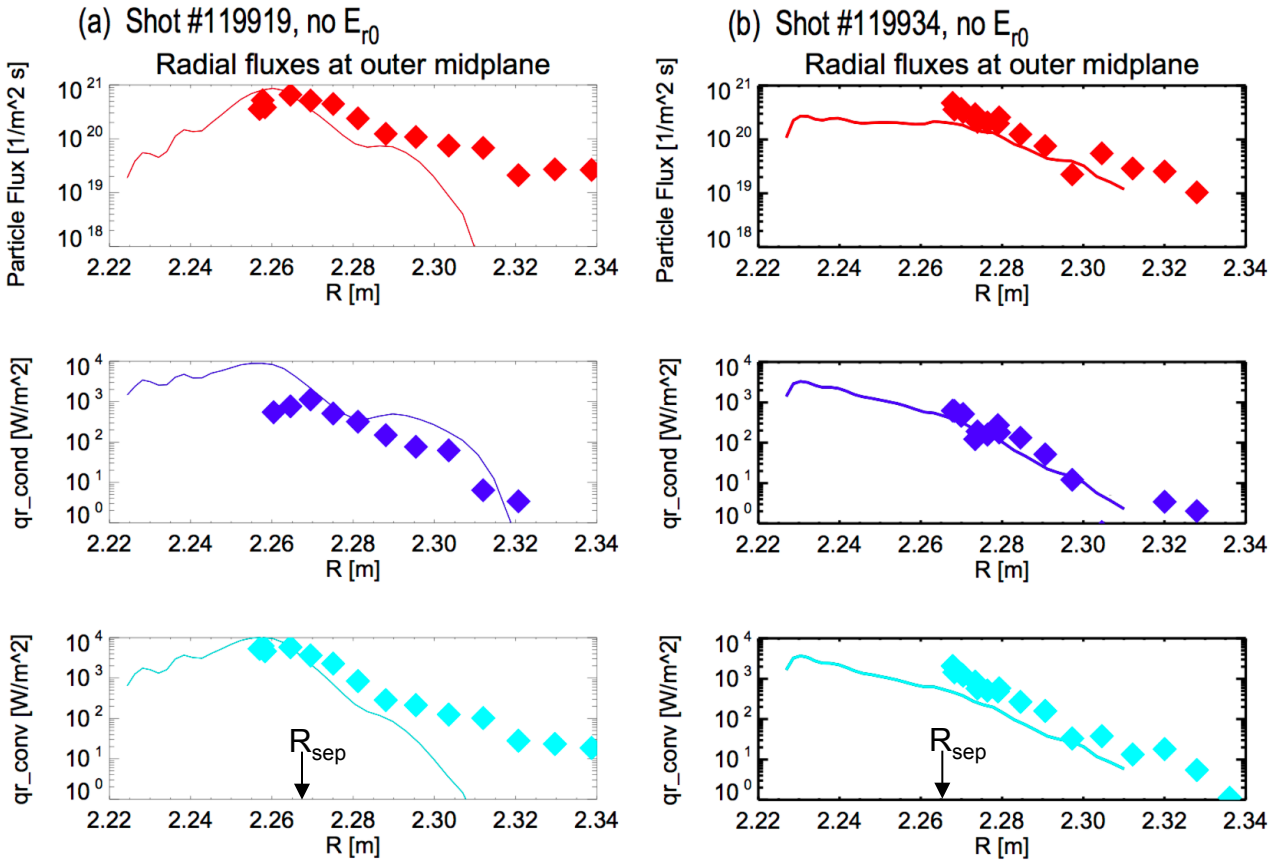

B. Cohen & Umansky, BOUT++2013 Workshop

Radial Electric Fields Fitted to Probe and CER Data for Simulations of Shots #119919, 119930 and 119934

- The electric potential and radial electric field are well determined from the probe data in the SOL, but tend to diverge and become unreliable inside the last closed flux surface
- The radial electric field determined by CER extends to smaller radii and shows that E_{radial} is relatively flat within significant temporal scatter

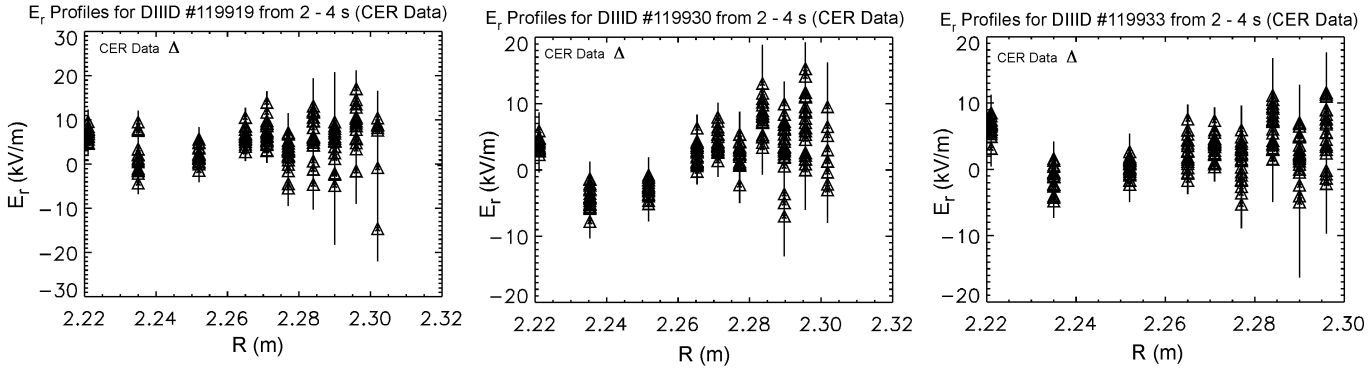

E_{radial} CER data

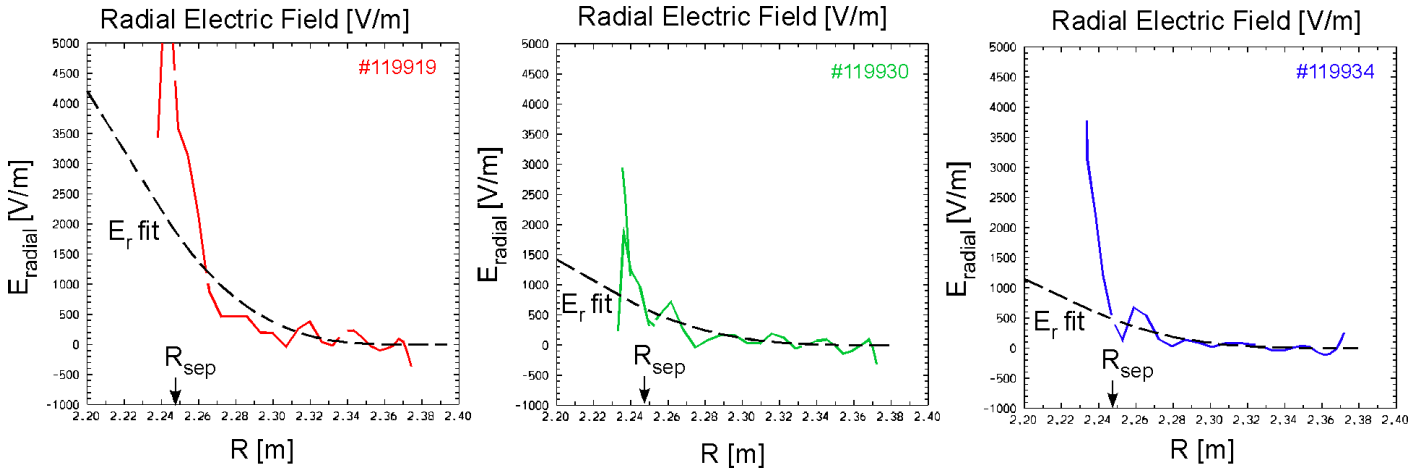

E_{radial} probe data & fit to probe/CER data

B. Cohen & Umansky, BOUT++2013 Workshop

Inclusion of Imposed Radial Electric Field Reduces Growth Rates and Saturated Fluctuation Levels in Simulation of Shot #119934

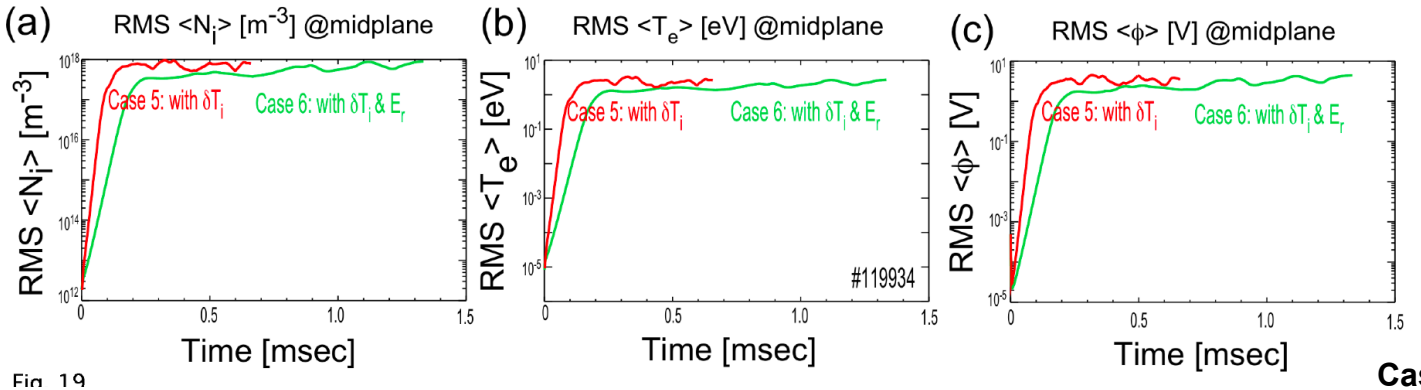

Fig. 19

Case 5 & 6a #119934

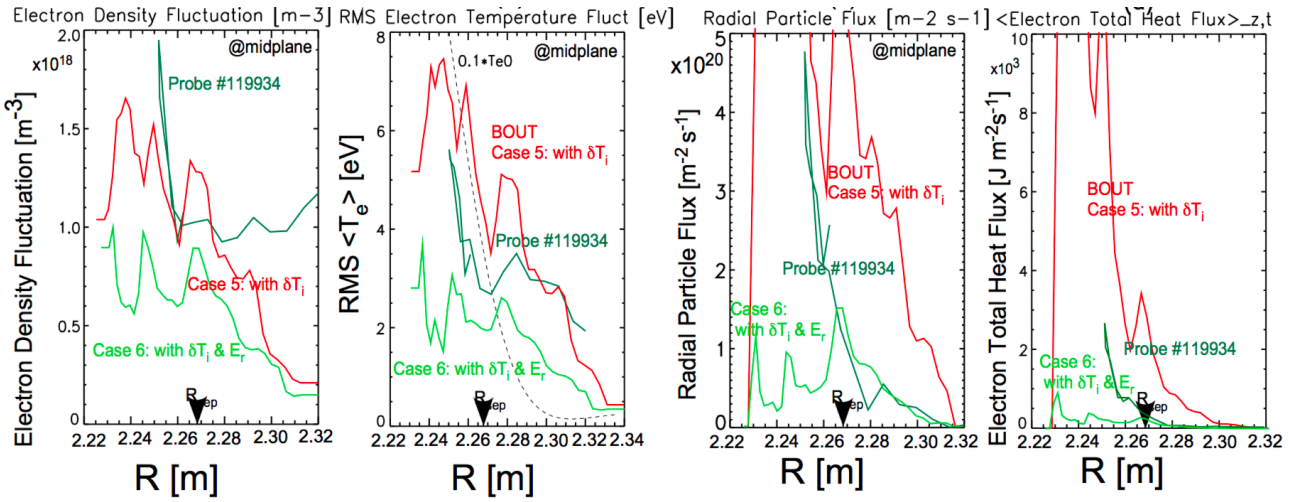

-- DIII-D expt
-- BOUT no Er
-- BOUT w Er

- Inclusion of E_r reduces linear growth rates and saturated fluctuation amplitudes less so; the finite E_r saturated amplitudes tend to recover to the levels of the E_r=0 case
- Simulation agreement with probe for relevant radii, 2.25m ≤ R ≤ 2.31m, remains fair

Evidence of Stabilizing Effects of Sheared Radial Electric Field with Reynolds Stress Zonal Flow Effects in Simulation of LAPD Edge Turbulence

- We simulate edge turbulence in LAPD cylindrical geometry with a 3-field electrostatic model supporting drift resistive instability (density, vorticity, electron temperature) including E_r and with/without zonal flow effects on the electric potential only, with density & temperature axisymmetric modes held constant to maintain "equilibrium" profiles fitting the experiment.

- We have compared simulations with imposed E_{r0} and with/without all zonal flows in the electric potential. Including all zonal flows reduces the saturated turbulence in the edge by a factor of 2 in the rms amplitudes over the time sampled.

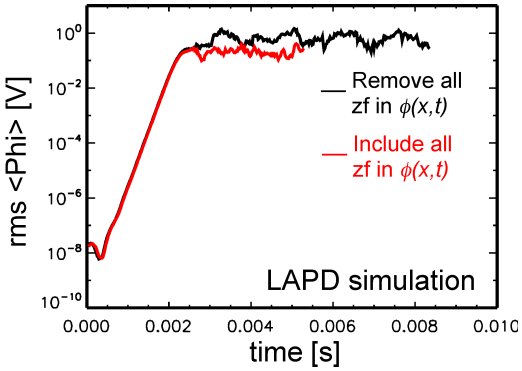

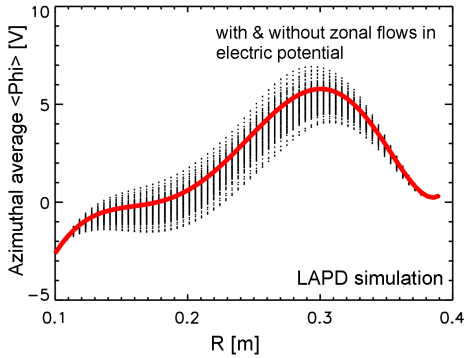

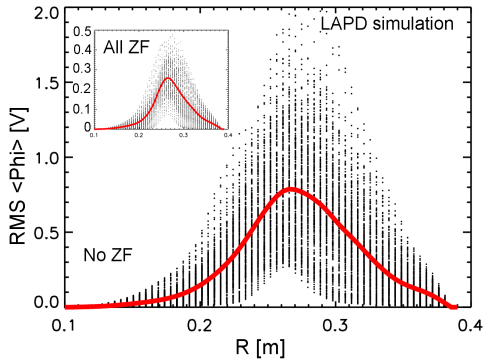

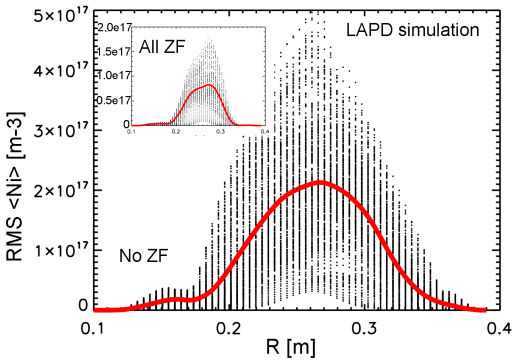

B. Cohen & Umans

Simulation results: Zonal flow correlates with turbulence amplitude in LAPD simulation

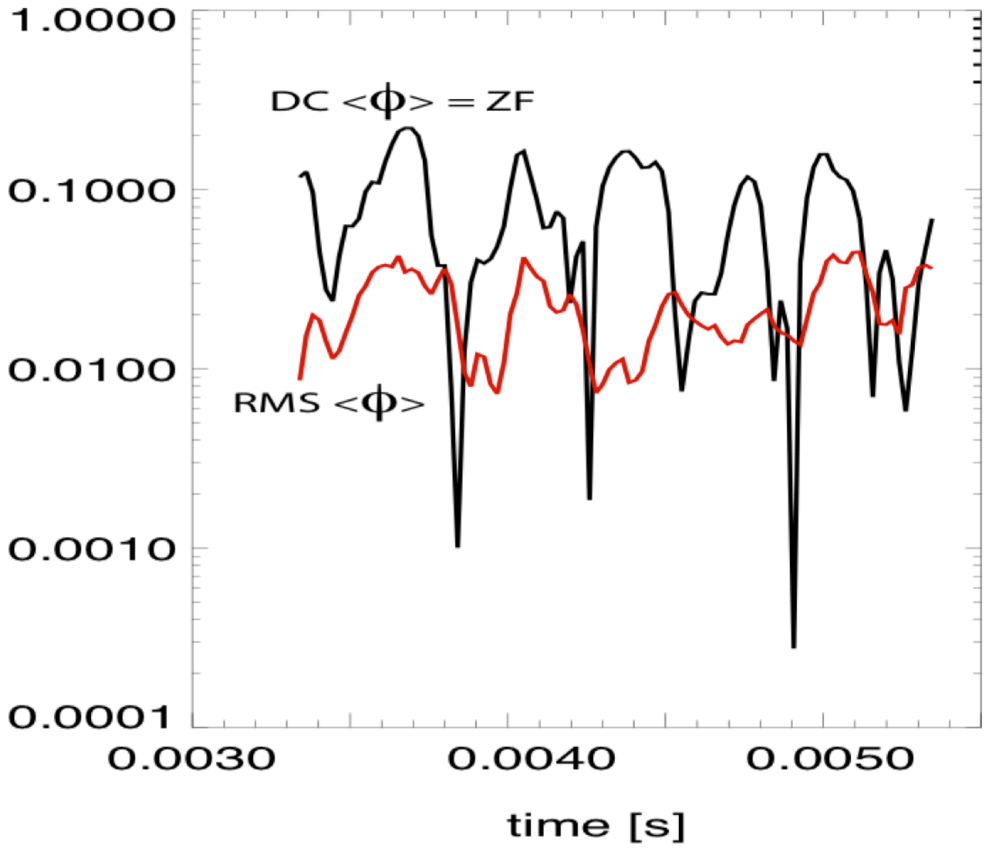

- **Apparently here ZF is not the only possible mechanism of turbulence saturation**
- **Coupling between unstable and damped n≠0 modes?**
- **Physics of turbulence saturation in LAPD is not yet understood**

Compare New Simulation Results with Self-consistent n=0 Zonal Flows in Vorticity Eqn and Fixed n=0 Density and Temperature Profiles to Earlier Results

- An equilibrium radial electric field E_0 is included in previous BOUT simulations for #119919 **Cases 1, 4, 5, & 6**, using fits to the experimental probe and CER data near midplane
- Imposed sheared ExB flow weakens linear growth rates, and saturation is much delayed (>2ms) and at lower amplitudes, while $5xE_r$ is much more stabilized.
- Inclusion of n=0 zonal flow in the vorticity eqn with fixed n=0 temperature and density profiles further reduces fluctuation amplitudes

With $T_{e,i}$ fluctuations

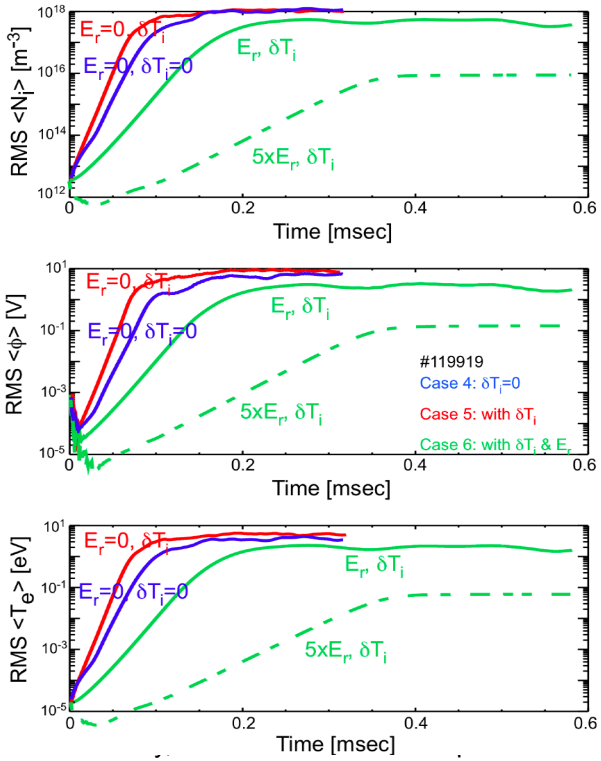

@midplane

With $T_{e,i}$ fluctuations and n=0 zonal flows in vorticity eqn

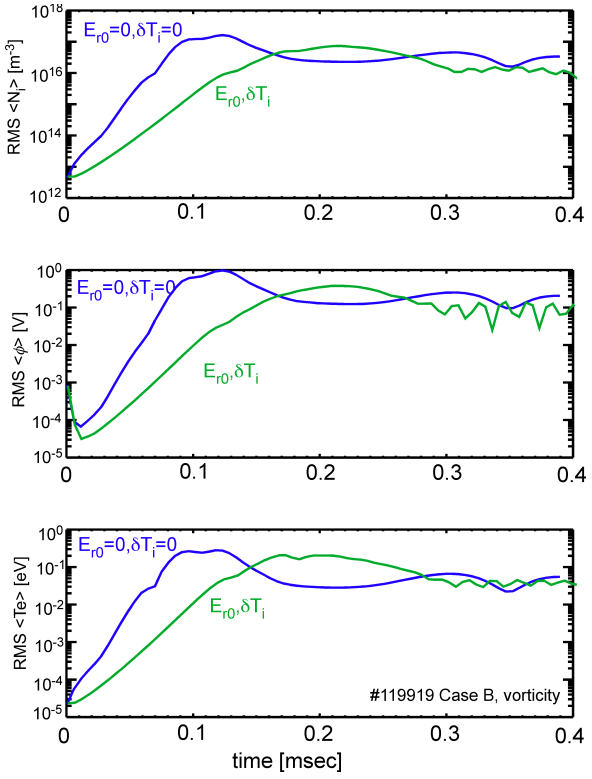

B. Cor

Fluctuation Ampitudes Are Further Reduced and Localized near Separatrix with Self-consistent n=0 Zonal Flows in Vorticity Eqn

- Inclusion of n=0 zonal flow in the vorticity eqn further reduces fluctuation amplitudes and localizes the density fluctuation
- n=0 temperature and density profiles are fixed

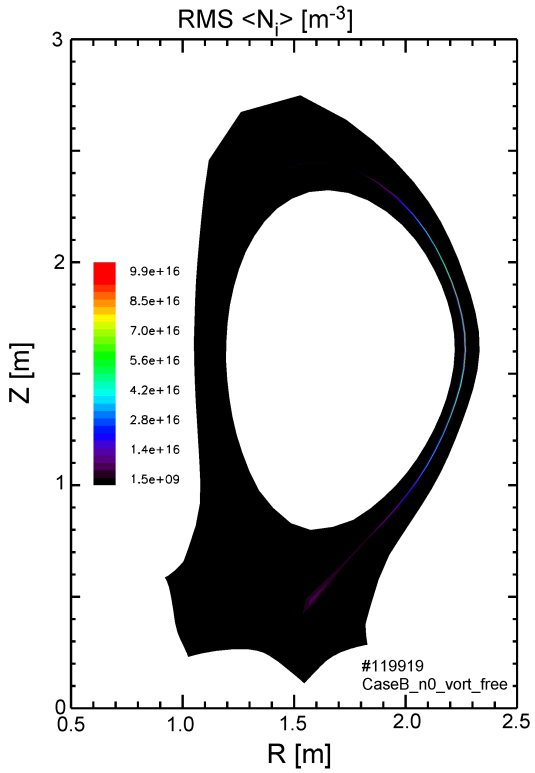

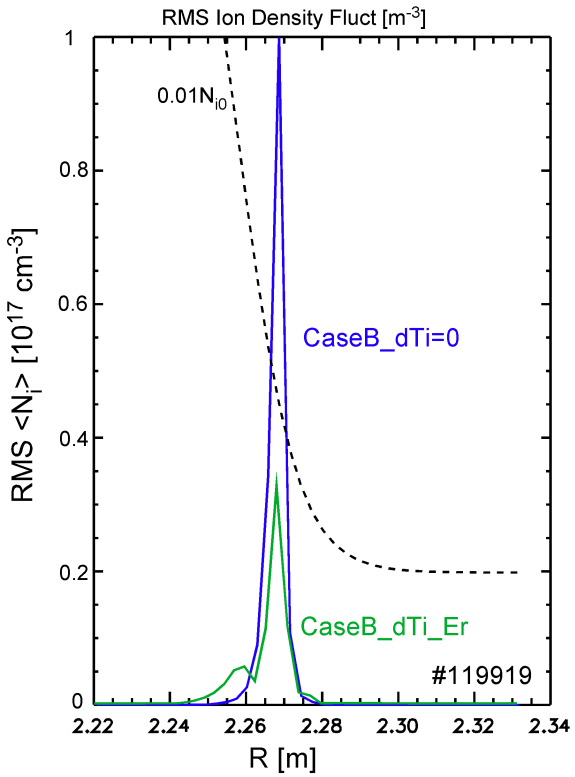

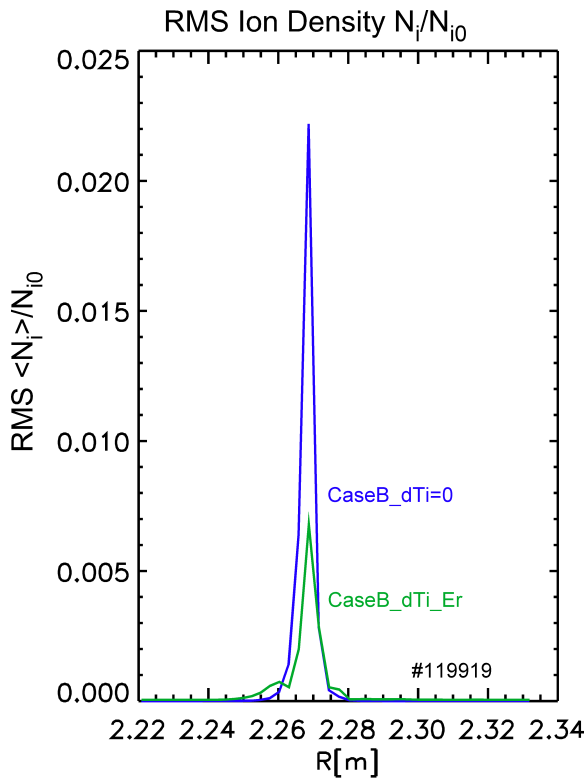

@ 0.4msec and in midplane

B. Cohen & Umansky, BOUT++2013 Workshop

Fluctuation Ampitudes Are Further Reduced and Localized near Separatrix with Self-consistent n=0 Zonal Flows in Vorticity Eqn

- Inclusion of n=0 zonal flow in the vorticity eqn further reduces fluctuation amplitudes and localizes the electron temperature fluctuation
- n=0 temperature and density profiles are fixed

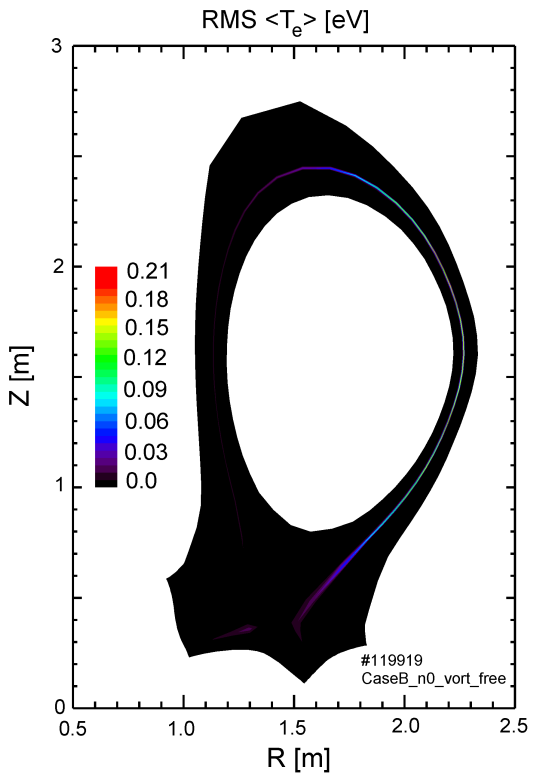

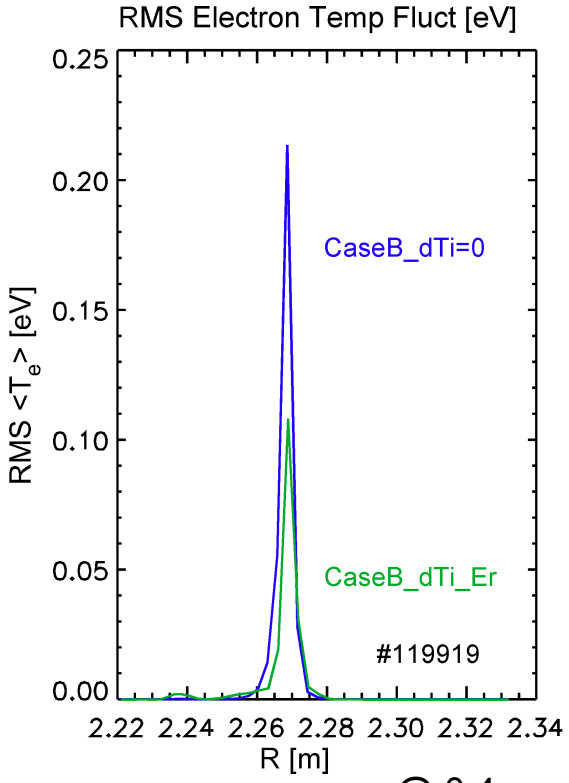

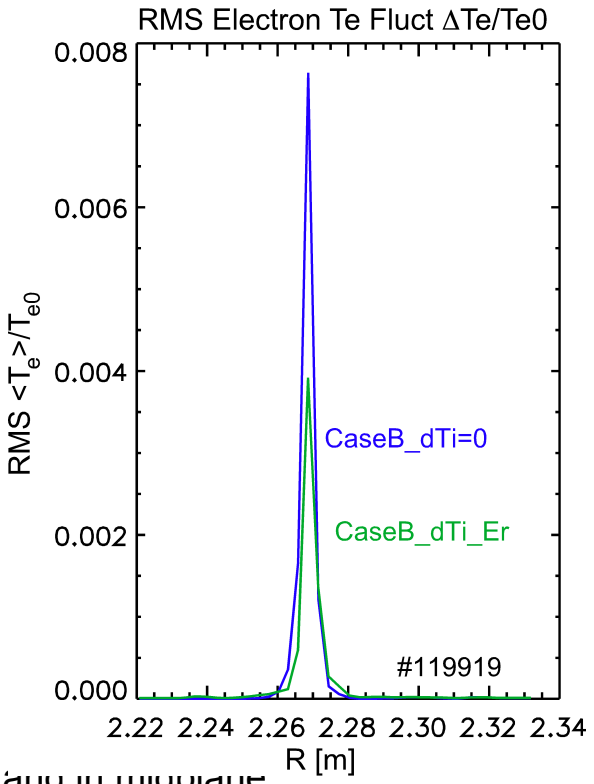

@ 0.4msec and in midplane

Work in progress: Including self-consistent evolution of n=0 modes in all fluid fields leads to fast growing "electrostatic Alfven mode" localized near inner target plate and negative density

Memorandum

From: MVU
To: file
Subject: Edge plasma MHD stability
Updated: Jul 27, 2013

Summary:

- Attempting BOUT-06 run with all profiles (i.e., n=0 components for all fluid fields) evolved, for DIII-D case 119919, we found that the run fails within a few steps with negative density.
- The cause is a rapidly growing axisymmetric mode localized near the inner target plate
- Apparently the cause is interplay of vorticity inversion and div(Jpar), similar to what is called sometimes the "electrostatic Alfven mode"

Case #1: BOUT06 produces expected resistive drift ballooning turbulence in full DIII-D X-point geometry

Encircled terms are dominant, balance each other

BOUT

$$\frac{\partial N_i}{\partial t} + (V_E + V_{\parallel}) \bullet \nabla N_i = \left(\frac{2c}{eB}\right) b_0 \times \kappa \bullet (\nabla P_e - N_i e \nabla \phi) + \nabla_{\parallel}(j_{\parallel}/e) - N_i \nabla_{\parallel} V_{\parallel i}$$

$$\frac{\partial \varpi}{\partial t} + V_E \bullet \nabla \varpi = 2\omega_{ci} b_0 \times \kappa \bullet \nabla P \quad + \quad N_i Z_i e \frac{4\pi V_A^2}{c^2} \nabla_{\parallel} j_{\parallel}$$

$$\frac{\partial V_{\parallel e}}{\partial t} = -\frac{e}{m_e} E_{\parallel} + \frac{1}{N m_e}(T_e \nabla_{\parallel} N_i) + 0.51 \nu_{ei} j_{\parallel}$$

$$\frac{\partial V_{\parallel i}}{\partial t} + V_E \bullet \nabla V_{\parallel i} = -\frac{1}{N_i M_i} \nabla_{\parallel} P$$

$$\mathbf{E} = -\tfrac{1}{c}\tfrac{\partial}{\partial t}\mathbf{A}_{\parallel} - \nabla\phi, \quad -\nabla_{\perp}^2 \mathbf{A}_{\parallel} = \tfrac{4\pi}{c}\mathbf{j}_{\parallel}, \quad \mathbf{B} = \nabla \times \mathbf{A}_{\parallel} + \mathbf{B}_0$$

$$\varpi = \nabla \cdot (e Z_i N_i \nabla \phi) \approx e Z_i N_i \nabla^2 \phi \quad \nabla_{\parallel} \approx \mathbf{b}_0 \cdot \nabla$$

NB: Cannot recover the expected relation between rho and phi in the inner leg!

B. Cohen, et al., Int'l Sherwood 2012

1

Fusion Energy Sciences

Including self-consistent evolution of n=0 modes in all fluid fields leads to fast growing "electrostatic Alfven mode" localized near inner target plate

Dispersion relation for the unstable mode

$$\begin{cases} \dfrac{\partial \varpi}{\partial t} + V_E \cdot \nabla \varpi = 2\omega_{ci} b_0 \times \kappa \cdot \nabla P + N_i Z_i e \dfrac{4\pi V_A^2}{c^2} \nabla_{\parallel} j_{\parallel} \\ \dfrac{\partial V_{\parallel e}}{\partial t} = \dfrac{e}{m_e} E_{\parallel} + \dfrac{1}{N m_e} (T_e \nabla_{\parallel} N_i) + 0.51 \nu_{ei} j_{\parallel} \end{cases}$$

Dominant terms encircled

$$\varpi = \nabla \cdot (e Z_i N_i \nabla \phi) \approx e Z_i N_i \nabla^2 \phi \qquad \nabla_{\parallel} \approx \mathbf{b}_0 \cdot \nabla$$

$$\begin{cases} -i\Omega[-eZ_i N_i (k_x^2 + k_z^2)\phi] = N_i Z_i e \dfrac{4\pi V_A^2}{c^2} (ik_{\parallel})(-eZ_i N_i) V_{\parallel e} \\ -i\Omega[V_{\parallel e}] = -\dfrac{e}{m_e}(-ik_{\parallel})\phi \end{cases}$$

$$\begin{cases} -i\Omega[(k_x^2 + k_z^2)\phi] = N_i Z_i e \dfrac{4\pi V_A^2}{c^2} (ik_{\parallel}) V_{\parallel e} \\ -i\Omega[V_{\parallel e}] = -\dfrac{e}{m_e}(-ik_{\parallel})\phi \end{cases}$$

Obtained linear dispersion relation.

If $k_{||}$ is complex (from the plots it seems to be) then there is instability

The growth rate is larger for smaller $k_z = n_{tor}/R$; axisymmetric mode is most unstable

Estimating $\Omega \sim 1e^{11} \times 1e^{-2} \times 1e^{-2} \sim 1e^{7}$ rad/s

$$-\Omega^2 (k_x^2 + k_z^2) = -\frac{e}{m_e} N_i Z_i e \frac{4\pi V_A^2}{c^2} k_{\parallel}^2 \qquad \Omega = \omega_{pe} \frac{V_A}{c} \sqrt{\frac{k_{\parallel}^2}{k_x^2 + k_z^2}}$$

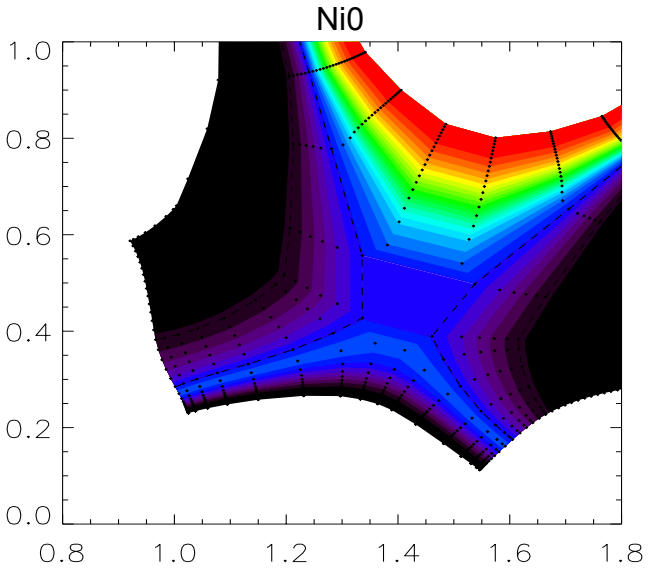

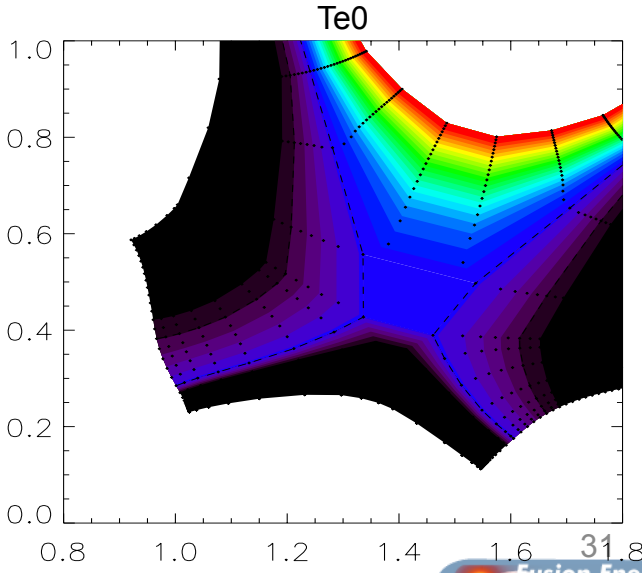

B. Cohen & Umansky, BOUT++2013 Workshop

Including self-consistent evolution of n=0 modes in all fluid fields leads to fast growing “electrostatic Alfven mode” localized near inner target plate

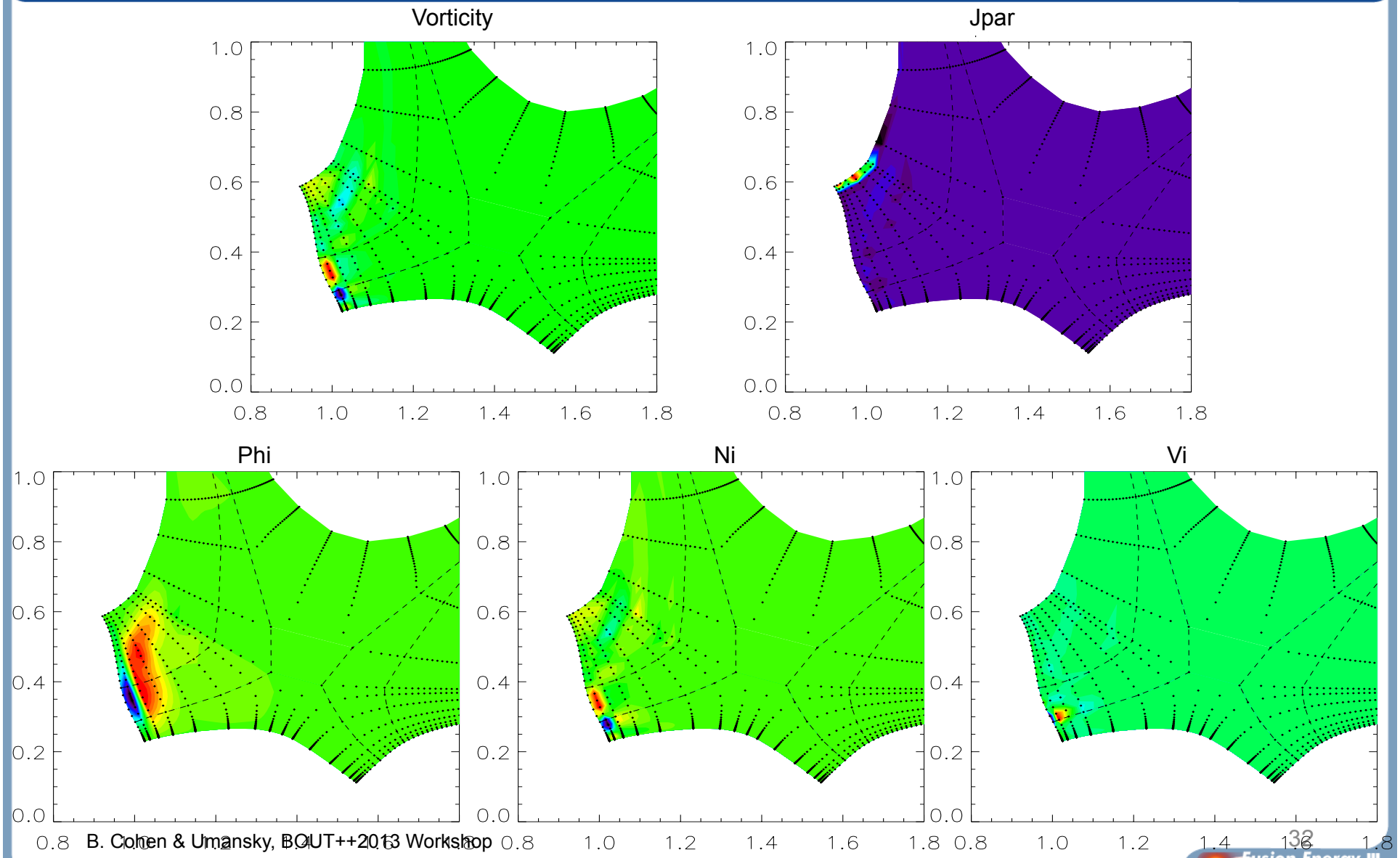

Including self-consistent evolution of n=0 modes in all fluid fields leads to fast growing "electrostatic Alfven mode" localized near inner target plate

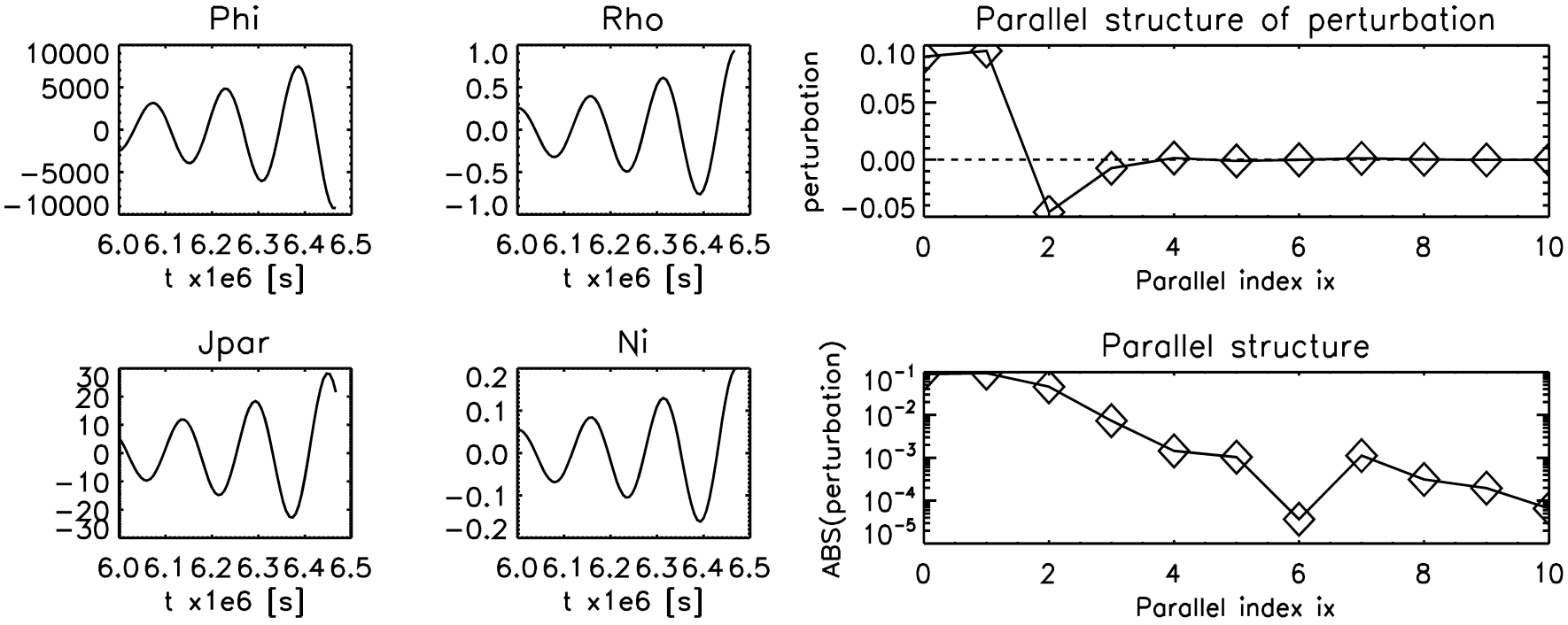

- The "electrostatic Alfven mode" is not unstable in gyrokinetic core simulaltions, and we doubt that the instability is physical here.
- We are experimenting with removing the electron inertia term to eliminate the "electrostatic Alfven mode."

Summary: Relative Agreement in Comparison of BOUT Results with DIII-D Probe and BES Data on Shots #119919 & 119934

- Comparison of suite of BOUT simulations to shots #119919/119921 probe and BES data: fluctuation frequency spectra, peak density amplitude radial half-width, correlation lengths, fluxes and diffusion rates are in reasonable agreement.
- RMS peak density and temperature fluctuation amplitudes measured with the Langmuir probe agree (#119919 & 119934) within factors of 2 or better with simulations as the physics model improves. Observed radial particle diffusivities and thermal conduction diffusivities in simulation are consistent with typical L-mode inferred values.
- There is factor-of-2 or better agreement seen between simulation synthetic diagnostics and the DIII-D #119921 BES data for the relative ion density and T_e fluctuation amplitudes, particle flux, spatial widths, and spectral frequency widths.
- Colder, lower density edge plasmas are less unstable and have smaller fluctuation levels.
- Inclusion of the radial E_{radial} inferred from experiment introduces a weakly sheared ExB flow that reduces growth rates and saturation amplitudes in simulations. But saturated amplitudes can recover nonlinearly, e.g., #119934.
- Study of self-consistent n=0 zonal flows is a work in progress
- **Drift resistive ballooning modes are a reasonable candidate for L-mode edge plasma turbulence in DIII-D shots #119919/21, #119930/34.**